





THESIS FOR THE DEGREE OF DOCTOR OF PHILOSOPHY

# Photochromism

Logic and Biologic Approaches

MARTIN HAMMARSON



**CHALMERS**

Department of Chemical and Biological Engineering

CHALMERS UNIVERSITY OF TECHNOLOGY

Gothenburg, Sweden 2013

Photochromism – Logic and Biologic Approaches  
Martin Hammarson

© Martin Hammarson, 2013

ISBN 978-91-7385-892-2

Doktorsavhandlingar vid Chalmers tekniska högskola  
Chalmers tekniska högskola  
Ny serie Nr 3573  
ISSN 0346-718X

Department of Chemical and Biological Engineering  
Chalmers University of Technology  
SE-412 96 Gothenburg  
Sweden  
Telephone +46-(0)31-772 1000

**Cover picture:** The binary photochromic light-switching of Spiropyran-DNA interaction: High DNA affinity (1) and low DNA affinity (0).

Chalmers Reproservice  
Gothenburg, Sweden 2013

# Photochromism

## Logic and Biologic Approaches

MARTIN HAMMARSON

Department of Chemical and Biological Engineering  
CHALMERS UNIVERSITY OF TECHNOLOGY

### Abstract

Photochromism is the light-induced colour change of molecules called photochromic compounds. The isomerisation causes changes in the electronic properties of the molecules and rearrangements of bonds which can be used in many more applications than the observed colour change. In this thesis photochromism has been used in molecular logic as well as biologic applications. In molecular logic the photochromic compounds have been used to realise logic gates which function in the same way as the traditional logic devices based on silicon found in any computer, the difference being that optical signals are used rather than electronic. The design and interpretation of a molecular memory and logic gates are presented. In biology, where often a binary *on-off* process is desired, DNA-binding of photochromic spiropyrans as well as their pH-dependent behaviour in aqueous solution are presented. Together these investigations are demonstrated as examples of how to use photochromism in logic as well as biologic applications.

**Keywords:** photochromism, molecular logic, DNA, DNA-binding, spiropyran, dithienylethene, photoswitch

# List of Publications

This thesis is based on the work contained in the following papers:

- I. **Photochromic Supramolecular Memory with Nondestructive Readout**  
Joakim Kärnbratt, Martin Hammarson, Shiming Li, Harry L. Anderson, Bo Albinsson and Joakim Andréasson  
*Angewandte Chemie – International Edition*, **2010**, *49*, 1854-1857
- II. **Molecular Implementation of Sequential and Reversible Logic Through Photochromic Energy Transfer Switching**  
Patricia Remón, Martin Hammarson, Shiming Li, Axel Kahnt, Uwe Pischel and Joakim Andréasson  
*Chemistry – A European Journal*, **2011**, *23*, 6492-6500
- III. **Molecular AND-logic for dually controlled activation of a DNA-binding spiropyran**  
Martin Hammarson, Johanna Andersson, Shiming Li, Per Lincoln and Joakim Andréasson  
*Chemical Communications*, **2010**, *46*, 7130-7132
- IV. **Characterization of the Thermal and Photoinduced Reactions of Photochromic Spiropyrans in Aqueous Solution**  
Martin Hammarson, Jesper R. Nilsson, Shiming Li, Tamás Beke-Somfai and Joakim Andréasson  
*Submitted to Journal of Physical Chemistry B*
- V. **DNA-binding Properties of Amidine Substituted Spiropyran Photoswitches**  
Martin Hammarson, Shiming Li, Per Lincoln and Joakim Andréasson  
*Manuscript*
- VI. **Photochromic Energy Transfer Switching on a DNA Scaffold**  
Martin Hammarson, Magnus Bälter, Shiming Li, Nittaya Gale, Tom Brown and Joakim Andréasson  
*Manuscript*

Related publication not included in this thesis:

## **Chiral Selectivity in the Binding of [4]Helicene Derivatives to Double-Stranded DNA**

Oksana Kel, Alexandre Fürstenberg, Nathalie Mehanna, Cyril Nicolas, Benoît Laleu, Martin Hammarson, Bo Albinsson, Jérôme Lacour and Eric Vauthey

*Chemistry – A European Journal*, **2013**, *19*, 7173-7180

## Contribution Report

Paper I	Designed and performed some of the experiments, analysed the results. Did not participate in the synthesis or the molecular modelling.
Paper II	Designed and performed most of the experiments. Analysed the results. Did not participate in the synthesis.
Paper III	Designed and performed all the experiments, analysed the results and wrote parts of the manuscript. Did not participate in the synthesis.
Paper IV	Designed and performed most of the experiments, analysed the results and wrote parts of the manuscript. Did not participate in the synthesis and theoretical calculations.
Paper V	Designed and performed the experiments, analysed the results and wrote the manuscript. Did not participate in the synthesis.
Paper VI	Designed and performed most of the experiments, analysed the results and wrote parts of the manuscript. Did not participate in the synthesis.

## Abbreviations

a.u.	arbitrary unit
bp	base-pairs
ct	calf thymus
DNA	deoxyribonucleic acid
DTE	dithienylethene
EET	excitation energy transfer
eq	equilibrium
HP	hydrolysis products
LD	linear dichroism
LD <sup>r</sup>	reduced linear dichroism
MC	merocyanine
MCH	protonated merocyanine
PSD	photostationary distribution
SP	spiropyran
SPH	protonated spiropyran
SVD	singular value decomposition
UV	ultraviolet
vis	visible



# Contents

<b>1</b>	<b>INTRODUCTION.....</b>	<b>1</b>
<b>2</b>	<b>BACKGROUND.....</b>	<b>3</b>
2.1	PHOTOCHROMISM.....	3
2.2	MOLECULAR LOGIC.....	4
2.3	DNA .....	5
2.4	PHOTOCHROMIC COMPOUNDS IN BIOLOGY .....	7
<b>3</b>	<b>THEORY AND METHODOLOGY .....</b>	<b>9</b>
3.1	INTERACTION BETWEEN LIGHT AND MATTER .....	9
3.2	ABSORPTION SPECTROSCOPY .....	10
3.3	LINEAR DICHROISM SPECTROSCOPY .....	11
3.4	FLUORESCENCE SPECTROSCOPY.....	12
3.5	ENERGY TRANSFER .....	14
3.6	PHOTOISOMERISATION .....	15
3.7	MOLECULAR COMPLEX FORMATION.....	15
<b>4</b>	<b>THE PHOTOCHROMIC MOLECULES.....</b>	<b>19</b>
4.1	SPIROPYRANS .....	19
4.2	DITHIENYLETHENES .....	22
<b>5</b>	<b>RESULTS.....</b>	<b>25</b>
5.1	PAPER I – A MOLECULAR MEMORY .....	25
5.2	PAPER II – A REVERSIBLE SEQUENTIAL LOGIC GATE .....	29
5.3	PAPER III – DNA-BINDING AS A LOGIC AND-GATE.....	33
5.4	PAPER IV – SPIROPYRANS IN AQUEOUS SOLUTION .....	36
5.5	PAPER V – DNA-BINDING OF AMIDINE SPIROPYRANS.....	40
5.6	PAPER VI – PHOTOSWITCHED ENERGY TRANSFER ON DNA .....	45
<b>6</b>	<b>CONCLUDING REMARKS.....</b>	<b>49</b>
<b>7</b>	<b>ACKNOWLEDGEMENTS.....</b>	<b>51</b>
<b>8</b>	<b>REFERENCES .....</b>	<b>53</b>



---

# 1 Introduction

---

**Photo** (from the Greek word φως, phos) *Light*

is one of the fundamental things of universe and earth. No light – no life. Understanding mechanisms on the molecular level hence requires the knowledge of the properties of light. Suggested by Albert Einstein<sup>[1]</sup> in the early 1900's, light is photons and can be described both in terms of wave and particle motion. Photons can affect the energy of a molecule, observed by us in numerous ways, from hazardous gamma radiation to invisible radio waves used in communication. The difference is the energy of light corresponding to the wavelength of the photons, which we, for visible light, refer to as the *colour* of the light.

**Chromism** (from the Greek word Χρώμα, chroma) *Colour*

is the interpretation of the human eye of light with different energy. For example, the colourful rainbow is the observed photons of different energy from the sun separated by the water molecules. White colour observed on earth is in fact a combination of photons ranging from purple/blue to red in energy. As water molecules reflect light differently depending on the energy, the result is the rainbow where all colours are observed from high-energy violet light to the lower energy red light. Other molecules also react differently to photons of different energy. One of these reactions based on the colour, is called *photochromism*.

**Photochromism**, *i.e.* “light-colour”, is the phenomenon where external light affects the colour of a material in a reversible manner such that the material changes colour after irradiation by light but returns to the original colour, either after irradiation from another light source or just being left in the dark over time. Far from all molecules are photochromic and the small subset displaying these properties are referred to as photochromic compounds.

In this thesis photochromism has been used as the basic tool to achieve function on the molecular scale of systems. Ultraviolet and visible light have been the main sources where the former is used in the colourisation reaction and the latter is used in the reverse reaction to the colourless form.

The aim of this work has been to use photochromic switching in molecular logic operations and to control biological functions. These are two initially separate fields that have many similarities today. Logic operations originate from the silicon-based electronic components. Molecular logic has been seen as a tool to enhance or replace the traditional silicon based devices by instead using molecules to switch binary from an *off*-state (0) to an *on*-state (1). The biological function in this thesis has been focused on water interactions as well as studying interactions with one of the most important biological molecules, the deoxyribonucleic acid, DNA. More specifically, the switching of the interaction to DNA is used in a binary *on-off* fashion.

This thesis shows results based on photochromism used in (i) molecular logic, (ii) molecular logic which operate in the biological field and (iii) pure biological field. First, two logic operations are presented: In Paper I and Paper II a photochromic dithienylethene and a photochromic spiropyran, respectively, have been used to interpret a memory device and a reversible sequential logic gate. A logic gate with biological applications, Paper III, follows this where the spiropyran was used as a

ligand to DNA. Due to the DNA-binding properties of the spiropyran, a characterisation of these compounds was made in aqueous solution and is presented in Paper IV followed by, in Paper V, a further characterisation of the DNA-binding properties of the isomers of selected spiropyrans. At the end, the DNA-binding property of the spiropyran is used to realise photo-controlled energy transfer switching on a DNA scaffold.

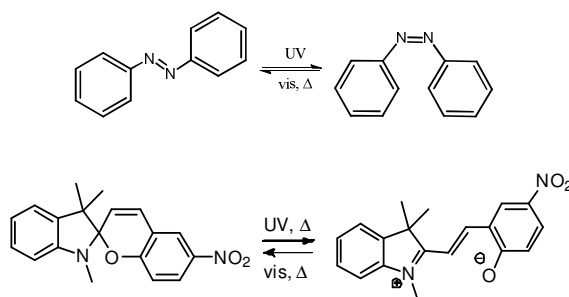
## 2 Background

This chapter gives an overview of photochromism, molecular logic, DNA and photochromism in biology. These are the central areas in this thesis.

### 2.1 Photochromism

As mentioned in the introduction, photochromism comes from the Greek words *phos* (light) and *chroma* (colour). These molecules are capable of reversible colour change by exposure to light<sup>[2]</sup> which generates a rearrangement of bonds, creating two different isomeric forms. Since the two forms generally have different physical and chemical properties, photochromic molecules have been used in everyday life. The most common example would be photochromic eyewear, which after exposure to UV light causes the normally transparent glasses to become darker.

Colour-change occurs everywhere in nature, hence it is not clear when photochromism first was observed and described. Still, the first colour change scientific paper dates back to 1866 when Fritzsche reported bleaching of an orange-coloured tetracene in daylight and the return to the coloured form when left in the dark.<sup>[2]</sup> In these studies, the scientific knowledge of molecular structure was not clear; hence, there were no large practical applications or designing. Later on, in the middle of the 20<sup>th</sup> century, the photochromism and *thermochromism*, colour-change due to thermal reactions, were well studied by Hirshberg and Fisher.<sup>[3]</sup> Now the first photochromic compounds were characterised such as the spiropyran which is used in this thesis.<sup>[4-5]</sup> Today, there are numerous different photochromic compounds characterised such as dithienylethenes, spiroxazines, azobenzenes and fulgimides.<sup>[6-7]</sup> Examples of photochromic compounds and their switching can be seen in Scheme 2.1.



**Scheme 2.1** Photochromic azobenzene switching (top) and the spiropyran switching (bottom). The azobenzene can be switched between *trans*-form to the left and the UV-light triggered *cis*-form to the right. The spiropyran can be switched between spiro form (left, SP) and the merocyanine form, (MC, right).

The photochromism effect is the result of a photoisomerisation, which is one of many pathways by which an excited molecule can relax. Other processes that will be presented later in this thesis involve emission of light called fluorescence as well as energy transfer. The photoisomerisation process rearranges the electronic cloud of the molecule which results in either a ring-opening or a rotation of a bond, *e.g.* *cis-trans* isomerisation. In the examples above, the azobenzene isomerisation is a bond-rotation while the spiropyran isomerisation is an example of a ring-opening process.

In this thesis there are two applications of photochromism presented. First, it is used in molecular logic and secondly, biological applications. The fields are based on different ideas but, as will be shown in this thesis, share many similarities.

## 2.2 Molecular Logic

Today, computers are part of almost everything we use in everyday life. Cars, mobile phones and refrigerators all contain small computerised devices. The reason for this massive development of computers can be explained by the development of the transistor, which is the smallest component in the computer today. These transistors are wired together to perform logic operations. 10 years after the introduction of the transistor in 1954,<sup>[8]</sup> Moore predicted the duplication of transistor density every 18-24 months, a prediction known as Moore's law.<sup>[9]</sup> In electronics, either a voltage is put through a circuit or it is not. This binary state, where a signal can be *on* – known as 1, or *off* – known as 0, is the basic property of every single computer. Moore's law has been proved to be valid for a very long time, longer than many people in the beginning thought. However, soon the top-down approach (going from a large object and making it smaller) may not be possible any more. An alternative way, the bottom-up principle, where you assemble small objects to make larger ones, has been discussed.<sup>[10]</sup> The smallest building blocks to start from today are the molecules (disregarding the atom-by-atom approach which is less likely to be successful in the foreseeable future).<sup>[11]</sup> Therefore, it is of interest to design molecules to perform logic operations and hence mimic the transistor and circuits in computers. The idea of a molecular logic gate was presented by de Silva in 1993.<sup>[12]</sup> Here, a fluorescent chromophore was attached to two quenchers. In the use of molecular logic, input signals are chosen as something that affects the system in a binary way. It may be chemical addition or light irradiation. The changes induced by the input signals are read out as output signals. In almost every case the output signals are not truly binary, but a certain threshold level is set, which means that anything below the level is read as 0 while everything above the level is read as 1. The output signals are often chosen to be fluorescence, the ability of molecules to emit photons after excitation. de Silva's device was a fluorescent anthracene derivative appended with two quenchers, which in its initial state was quenched. Only by addition of  $\text{Na}^+$  ions together with protons can the fluorescence reach above the threshold level.<sup>[12]</sup> This was interpreted as a molecular AND logic gate meaning that in order to see fluorescence both input 1 ( $\text{Na}^+$  ions) and input 2 ( $\text{H}^+$  ions) must be added. If only one of the chemicals is added, no fluorescence is observed. The logic operations are described by a truth table where all input combinations and the resulting output are presented as well as a graphic symbol (Figure 2.1). Several different logic gates have later been presented.<sup>[13-17]</sup> Furthermore, molecules have been designed and synthesised to perform functions that are typically performed by complex logic circuits, *i.e.* several logic gates wired together, such as half-adders,<sup>[18-20]</sup> encoders and decoders.<sup>[21-22]</sup>

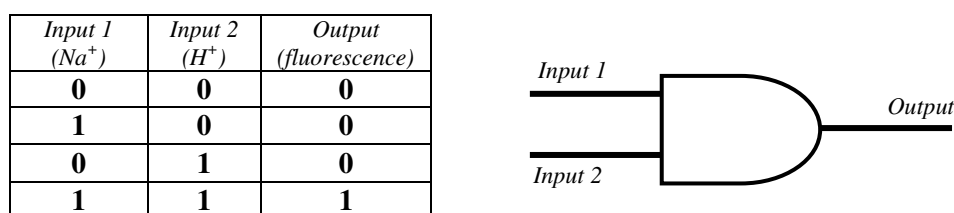


Figure 2.1. A molecular AND gate and its truth table.

Photochromic compounds serve as a good example of molecules which can be chosen to perform logic operations, often covalently linked to a fluorescent reporter chromophore.<sup>[23-25]</sup> Since this colour change only requires light as input and not any chemical addition, they have proven useful in molecular logic because they are easier to set and reset and do not suffer from dilution problems. Also there is no build-up of chemical waste-products that can be a result of chemical addition.

Although molecular logic was developed aiming at the potential replacement of silicon based transistors, it may not only be used for this purpose. The binary responses can easily be transferred to biology. An illustrative example may be the principle of an anticancer drug. Treatment against cancer requires knowledge of the cancer cells: how to detect them and how to distinguish them from healthy cells but most of all, how to kill them while optimally leaving all other cells unaffected. The induction of cell death can be seen as a binary output by a molecular anticancer drug (kill or not kill), with inputs designed to distinguish cancer cells from other cells. It has therefore been suggested that the use of molecular logic may not have its most immediate use in the computer world, but instead in the biological world, where the silicon-based technology cannot be used. The use of molecular logic in biological applications has some recent examples.<sup>[26-29]</sup> One example is reported by Akkaya and co-workers who designed a molecule that when excited stimulated the production of singlet oxygen ( $^1\text{O}_2$ ), a known cell poison. However, in the absence of inputs ( $\text{Na}^+$  ions and protons), the production of singlet oxygen is very low and was only turned on if the amount of  $\text{Na}^+$  and protons were sufficiently high.<sup>[30]</sup> As cancer cells and their surroundings tend to be more acidic<sup>[31-32]</sup> and have a higher concentration of  $\text{Na}^+$ ,<sup>[33]</sup> the production of singlet oxygen is only obtained when these prerequisites are fulfilled, something not to be expected in normal cells. This serves as a good example of a biological AND gate where the drug itself is affected by its environment in a selective way, something which is very desirable in drug development.

## 2.3 DNA

---

In this thesis DNA is the main biological macromolecule. Hence, this section will cover the basics of its structure. This will be followed by a section, which covers the photochromism in biology in general and in DNA in particular.

DNA is one of the fundamental elements of life and the storage place of the genetic information. The central dogma of life which was proposed by Crick in 1958,<sup>[34]</sup> is the basis for our understanding of the living cells: DNA is transcribed into RNA which is translated into a protein. DNA is a double stranded polymer of alternating sugar and phosphate groups held together in a helical structure by hydrogen bonding between bases attached to the sugars. The monomer is called a nucleotide and is built up by deoxyribose sugar covalently attached to one of the four fundamental bases, adenine (A), guanine (G), cytosine (C) and thymine (T). The fundamentals of the genetic code are the different bases which hydrogen bond in a specific pattern exclusively, A to T and G to C, according to the hypothesis first presented by Watson and Crick in 1953.<sup>[35]</sup> The structure and pairing of the bases can be seen in Figure 2.2.

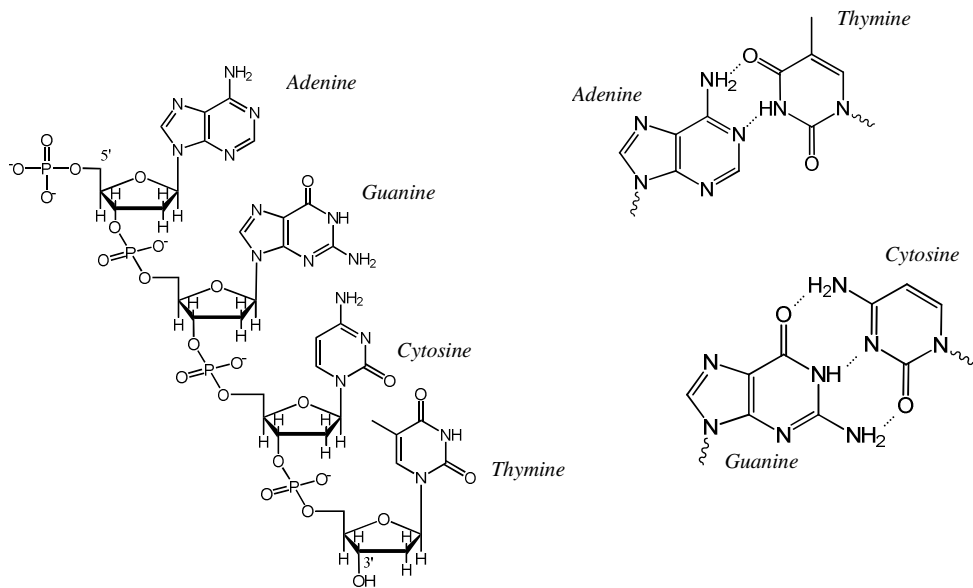


**Figure 2.2.** The structure of a single stranded DNA with sugar-phosphate backbone and the four different bases (left) and the Watson-Crick base-pairing which holds together the double strand (right).

Phosphodiester bonds hold the single strand together with each phosphate carrying one net negative charge. The resulting double helix is a large polyanion at physiological pH. The stability of the helix is strongly dependent on cation concentration and hydrogen bonding of water on the surface, as well as the hydrophobic interaction between the bases in the middle of the helix. The double helix is a right handed non-symmetrical spiral with its structure strongly affected by its environment. In an aqueous environment (as in any biological system), the B-form structure, seen in Figure 2.3, dominates.

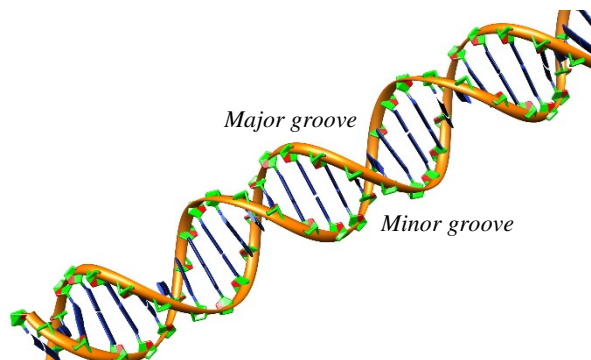


**Figure 2.3.** The 3D structure of the in aqueous solution dominating B-form of the DNA double helix with its minor and major groove.



In this form, on the surface of the helix there are two grooves distinguishable, one large, 22 Å wide, called the major groove and one smaller, 12 Å wide, called the minor groove.<sup>[36]</sup> In this thesis the binding of photochromic spiropyrans to DNA has been studied. Non-covalent reversible interactions with the DNA helix can in principle be of four kinds: (i) Electrostatic interaction with the anionic sugar-phosphate backbone, (ii) intercalation between the bases inside the helix, (iii) interaction in the major groove and (iv) interaction in the minor groove. The large polyanion structure of DNA is surrounded by cations that stabilises the helix. The binding of a charged ligand to DNA has been shown to be strongly dependent on the ionic concentration and decreases with addition of NaCl.<sup>[37]</sup> For a high binding constant the salt concentration should therefore be minimal and the net charge of the binding species should be positive. The cellular concentrations of cations are, however, rather high. A normal concentration of K<sup>+</sup> ions is 140 mM and Na<sup>+</sup> is 5-15 mM. Together with Ca<sup>2+</sup> and Mg<sup>2+</sup> the total ionic strength in the cell will therefore be roughly 160 mM.<sup>[38]</sup> For intercalation between the bases, the molecule should also be planar with a hydrophobic centre, where a typical example is the intercalating ethidium bromide seen in Figure 2.4.

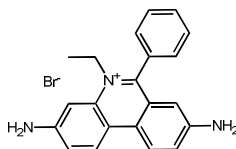


Figure 2.4 Ethidium bromide intercalator of DNA

## 2.4 Photochromic Compounds in Biology

Through-out human history, there has always been a mystery how the world actually works and why. Even though science may never explain why things are as they are, our understanding has been vastly improved in the last 100 years. But the more answers we get, the more questions arise. Today, we know the structure and function of biological molecules such as DNA described above. We also know a lot about and continuously gain knowledge of protein structures in our cells. However, there are still many complex reactions going on in the world of molecules which we are far away from understanding. Will we ever understand all processes in biology fully in such a way that every illness can be cured and all diseases eradicated? Perhaps not, but concentrated research in specific areas slowly takes us one step at the time closer towards this goal.

The present science is focussed on molecular structure and function *i.e.* why ligand interactions are formed and how cellular function is affected. The research hence requires more and more knowledge of the molecular properties of substances and design and functionality of this. As photochromic molecules are small compounds, which change structure dramatically in a mostly non-destructible way, by irradiation of light, it may be very useful in the biological context. As mentioned earlier, molecular logic has been moved into biology, as it is often desired in biology to have a binary *on-off* switch for a specific process. These processes occur everywhere in cells and involve DNA, RNA and proteins but with more knowledge of DNA structure it is one of the most prominent targets for biological applications.

In recent years, there are many examples of light-switched effects on DNA. Light-switched molecules have been attached to the DNA-bases to control the interaction of proteins with DNA as well as the properties of the helix. Modifying a base by attaching a photochromic azobenzene has been shown to control the stability and hybridisation of the double helix.<sup>[39-41]</sup> This has in turn been used to stop the

polymerase from replication further downstream in the sequence because of the steric hindrance caused by the isomer. But the replication can be activated by photo-induced isomerisation.<sup>[42]</sup> The same molecule has also been used to photo-regulate transcription by promoter binding.<sup>[43]</sup> Another photochromic unit, a diarylethene based molecule has also been incorporated into DNA for hybridisation control<sup>[44]</sup> or a photochromic motif to a protein ligand.<sup>[45]</sup> One drawback of these projects is that they have required synthetic modification of bases or ligands by covalent attachment of photochromic molecules. To be suitable for living organisms and for *e.g.* cancer treatment, one must surmount the need of covalent pre-modification of the targeted DNA-molecules. This field has increased in the recent time. Examples involve light-controlled RNA molecule interaction<sup>[46]</sup> as well as irreversible generation of a DNA binding derivative.<sup>[47]</sup> Nakatani and co-workers have designed azobenzene moieties which are not attached to the DNA strand itself. Instead, it is a linker which can base-pair with guanines in the helix<sup>[48]</sup>. The result is a molecular glove as two mismatched single strands of DNA could be matched and hybridised and dehybridised by use of light,<sup>[49]</sup> something which also was extended to asymmetrical ligands.<sup>[50]</sup>

In our lab the spiropyran was found to bind in a light-controlled fashion.<sup>[51]</sup> We therefore moved forward with more DNA-binding studies which is a basis for this thesis. Apart from this, the spiropyran has been shown to be able to penetrate membranes<sup>[52]</sup> as well as having photo-controlled cytotoxic effects on cells.<sup>[53]</sup>

There are also many more examples of light-controlled tools, caging and switching in biological applications. The interested reader may find more information in the many reviews that are available.<sup>[54-56]</sup>

---

## 3 Theory and Methodology

---

*This chapter explains some of the fundamental theory and methodology used in this thesis. Central parts are absorption, linear dichroism, fluorescence, energy transfer, photoisomerisation as well as molecular complex formation.*

### 3.1 Interaction between Light and Matter

---

Light or electromagnetic radiation is an oscillating wave of an electric and a magnetic field oriented perpendicular to each other and to the direction of propagation. The oscillating electric field can interact with the electrons in a molecule and induces oscillations in the electron cloud surrounding the atoms. If the electron cloud is polarisable in the same direction as the polarisation of the incoming electric wave, a transition can occur. It is a forced transient oscillation of the cloud which rearranges the charge distribution in the molecule and gives rise to a different electronic state of the molecule. The molecule becomes excited, from an initial state,  $i$ , to a final state,  $f$ . For this transition to occur the *Bohr frequency condition* must be satisfied, *i.e.* the energy of the light must correspond to the energy difference between the final and the initial state

$$\Delta E = E_f - E_i = h\nu = \frac{hc}{\lambda} = hc\tilde{\nu} \quad (1)$$

In this equation the energy,  $E$ , of the light is described by either a frequency,  $\nu$ , wavelength,  $\lambda$  or wavenumber,  $\tilde{\nu}$ ,  $h$  is Planck's constant and  $c$  is the speed of light.

The ability of the molecule to be excited is approximately described by the electronic transition dipole moment vector,  $\vec{\mu}_{fi}$ , which is defined by

$$\vec{\mu}_{fi} = \int \psi_f^* \hat{\mu} \psi_i d\tau \quad (2)$$

where  $\psi_f^*$  and  $\psi_i$  are the electronic wavefunctions in the final and initial state, respectively,  $\hat{\mu}$  is the electronic dipole moment operator and the integration is made over whole space ( $d\tau = dx dy dz$ ).

The probability of the incoming light to be absorbed, *i.e.* induce a transition between the two states is hence proportional to the magnitude of the transition dipole moment as well as the orientation of it relative to the polarisation direction of the incoming light. With this orientation difference described by the angle  $\theta$ , the absorption of the sample,  $A$ , can be described by

$$A \propto |\vec{\mu}_{fi}|^2 \cos^2 \theta \quad (3)$$

When a molecule is excited to a higher state it will after a short period of time return to its ground state by different processes. The possible routes are depicted in a *Jablonski diagram* (Figure 3.1) where the arrows indicate the transitions between different states.

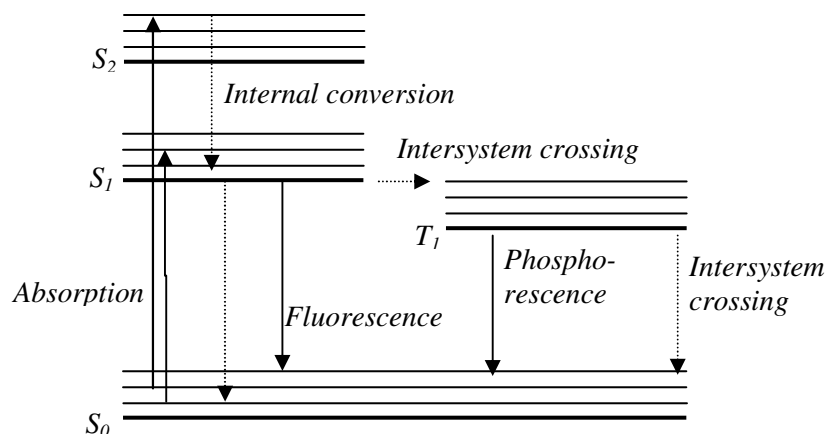


**Figure 3.1.** A Jablonski diagram showing the processes involved after excitation of a molecule.

After excitation the molecule ends up in one of the excited states  $S_n$  ( $n = 1, 2, 3, \dots$ ). From here the vibrational relaxation and internal conversion processes are normally by far the most efficient deactivation route and the excited molecule returns to the lowest singlet excited state ( $S_1$ ). From here the molecule can return to its ground state  $S_0$  by radiative or non-radiative decay mechanisms. The radiative decay from the singlet excited state is known as fluorescence and is a process often on the pico- to nanosecond timescale. Non-radiative decay is mostly internal conversion, which is by far most common, but another path is through intersystem crossing to an excited triplet state ( $T_1$ ). This process changes the spin-state of the molecule and according to quantum mechanics it is forbidden, which therefore makes the process slow and unlikely. From the triplet excited state, the radiative decay to the singlet ground state is called phosphorescence which is a much slower process typically on the millisecond to second timescale. It may also return to the ground state through vibrational relaxation and intersystem crossing in a non-radiative process.

There are other deactivation pathways for electronically excited molecules and in this thesis two processes are described: A nearby molecule can gain the energy of the excited molecule, a process known as energy transfer (*vide infra*) or, the molecule itself changes structure in the excited state and is relaxed down to a new ground state with another molecular structure, the phenomena known as photoisomerisation which is the process of photochromism.

## 3.2 Absorption Spectroscopy

The measurement of the photon absorption of a molecule is known as absorption spectroscopy. By measuring incident and transmitted light intensities ( $I_0$  and  $I$  respectively) when light is passed through a sample with a path length  $l$ , the absorbance can be calculated according to the *Beer-Lambert law*,

$$A(\lambda) = \log \frac{I_0}{I} = \varepsilon(\lambda)cl \quad (4)$$

where the absorbance,  $A$ , is proportional to the concentration of the sample,  $c$ , and the path length,  $l$ . The proportionality constant,  $\varepsilon$ , is called the molar absorption coefficient (molar absorptivity) and depends on the wavelength of the light,  $\lambda$ , as well as the magnitude of the electronic dipole moment.

Absorption spectroscopy is a very useful technique for concentration determination when the molar absorption coefficient is known. It depends on the molecule itself as well as the environment surrounding the molecule and hence spectral changes observed in absorption spectroscopy can be used to study molecular interactions or environmental change due to such an interaction. This technique is also the easiest way to measure photochromism where the absorption of the sample is measured under constant irradiation of a stronger light source which isomerises the molecule.

### 3.3 Linear Dichroism Spectroscopy

In conventional absorption spectroscopy no consideration is taken of the orientation of the incoming light wave and the molecule. In *Linear Dichroism* spectroscopy however, the absorption of polarised light is measured and the orientation dependent absorbance is measured. Linear Dichroism, LD, is defined as the differential absorption of light polarised parallel,  $A_{\parallel}$ , and perpendicular,  $A_{\perp}$ , to a macroscopic orientation axis:

$$LD = A_{\parallel} - A_{\perp} \quad (5)$$

If a molecule is oriented so that its electronic dipole moments is found at a specific angle relative to the polarisation of the light, the sample will give rise to an LD signal (the absorption is proportional to the cosine square of the angle between the electric field of the light and the electric dipole moment, see equation 3). If the angle of the electric dipole moment is known, the orientation of the molecule relative to the macroscopic orientation axis can be determined by the Reduced Linear Dichroism,

$$LD^r = \frac{LD}{A_{iso}} = \frac{3}{2}S(3\cos^2\alpha - 1) \quad (6)$$

which is defined as the LD normalised by the isotropic absorbance,  $A_{iso}$ . In this equation, which is valid only for rod-like molecules,  $\alpha$  is the angle between the electric dipole moment of the molecule and the macroscopic orientation axis.  $S$  is a scaling factor called the orientation factor. It is defined as the efficiency of the macroscopic orientation and can have values between 1 and 0 where  $S = 1$  expresses the sample being perfectly oriented with the macroscopic orientation axis and  $S = 0$  means a complete random orientation.<sup>[57]</sup>

Orientation of a sample can be achieved in different ways. In this thesis the orientation is obtained by rotation of the sample cell, making elongated particles orient by the viscous flow. In a couette cell (Figure 3.2), the liquid sample is between an inner and outer cylinder in a gap of 0.5 mm. Rotating one of the cylinders, in this case the outer one, creates a shear flow gradient between the cylinders that causes long elongated particles to align in the flow direction.<sup>[58]</sup>

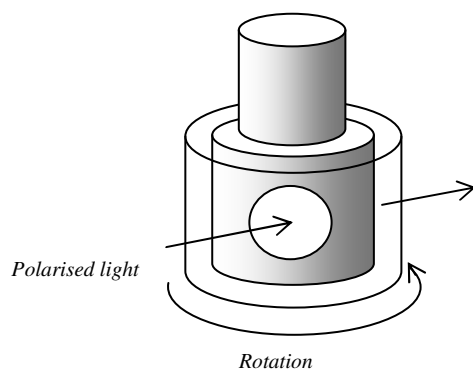


**Figure 3.2.** The principles of a couette cell. The sample is kept between two cylinders and the outer one is rotating. Polarised light is sent through the sample and collected on the other side and an LD signal can be measured.

The DNA double helix is a long rod-like structure large enough to be oriented and as the DNA bases are oriented perpendicular to the helix orientation, the LD of DNA is negative. For the distinct DNA absorption band at 260 nm, caused by absorption of the four bases, the orientation factor ( $S$ ) can be calculated by assuming  $\alpha$  to be  $90^\circ$ . Molecules under a certain size are not affected by the shear flow gradient and are instead randomly oriented in the cell. However, if the small molecules interact with the large ones, *e.g.* by binding, they will be trapped in the large molecules in a specific orientation and will give rise to an LD signal. It is therefore possible to use LD as a method to measure binding of ligands to DNA. By determining the isotropic absorbance of the binding species, the reduced LD can be calculated and can be used to give knowledge of the possible binding mode. For example, the well-known intercalator ethidium bromide mentioned earlier (Figure 2.4) gives rise to a negative LD with an  $LD^r$  very close to the DNA bases. A minor groove binding ligand will be oriented more parallel to the DNA helix ( $\alpha = 45^\circ$ ) and shows a positive LD. As a consequence, LD is a very useful technique for studying DNA-binding if the molecule absorbs in a wavelength region above the absorbance of the DNA ( $> 300$  nm) and displays a clear and broad spectrum. Naturally, this is not always the case, which can limit the use of LD.

### 3.4 Fluorescence Spectroscopy

The measurement of photon emission from an electronically excited molecule is called fluorescence spectroscopy. All molecules can absorb photons, but far from all of them emit intense fluorescence. The emission properties depend on the different rates of the deactivation pathways from the first singlet excited state,  $S_1$ , down to its ground state,  $S_0$ . The fraction of molecules which return to its ground state by fluorescence is the same as the ratio between emitted and absorbed photons and is called fluorescence quantum yield,  $\phi_f$ , given by

$$\phi_f = \frac{\text{photons emitted}}{\text{photons absorbed}} = \frac{k_f}{k_f + k_{ic} + k_{isc} + k_Q} \quad (7)$$

where  $k_f$ ,  $k_{ic}$ ,  $k_{isc}$  are the rate constants of fluorescence, internal conversion and intersystem crossing respectively,  $k_Q$  is the quenching constant introduced to account for quenching processes such as energy- and electron transfer reactions with nearby molecules. The quantum yield of fluorescence is often determined by

relating the fluorescence intensity to a reference compound with known quantum yield according to

$$\phi_f = \phi_{f_R} \frac{I}{I_R} \frac{A_R}{A} \frac{n^2}{n_R^2} \quad (8)$$

where  $I$  is the integrated emission intensity,  $A$  is the isotropic absorbance at the excitation wavelength and  $n$  is the refractive index of the solvent used, all for the fluorophore studied as well as the reference compound ( $R$ ) with known quantum yield.

The lifetime of the excited state,  $\tau$ , is defined as the average time the molecule spends in the excited state and is given by

$$\tau = \frac{1}{k_f + k_{ic} + k_{isc} + k_Q} \quad (9)$$

Fluorescence spectroscopy can be performed by steady-state and time-resolved measurements which together can give information of the quantum yield and lifetime.

In steady-state fluorescence spectroscopy, the sample is constantly excited by light and an emission spectrum is recorded. The fluorescence intensity and the shape of the corresponding spectra are sensitive to the environment making it a good tool to study molecular interactions. Fluorescence spectroscopy is a very sensitive technique which can be used for extremely low sample concentrations, even on the single molecule scale. Thus it has been widely used in molecular logic because in theory it requires only one molecule per bit information. However, since the fluorescence quantum yield very rarely is 1, in reality you will always need an ensemble of molecules.

In time-resolved fluorescence spectroscopy the sample is excited with a short pulse of light, usually a laser pulse, and the fluorescence intensity decay over time is measured. The technique used in this thesis is called *Time-Correlated Single Photon Counting* (TCSPC). The population of molecules in their excited state decrease according to a first order kinetics

$$\frac{dn(t)}{dt} = -n(t) \sum k \quad (10)$$

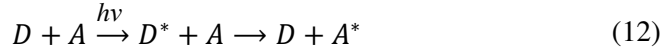
where  $n(t)$  is the number of excited molecules and  $\sum k$  is the sum of all rate constants involved in the deactivation of the excited state (see equation 7). As the excited state population is proportional to the intensity,  $n(t)$  can be replaced by the intensity in the above equation and the solution becomes

$$I(t) = I_0 e^{-t \sum k} = I_0 e^{-t/\tau} \quad (11)$$

from which the fluorescence lifetime can be determined. In this thesis, time-resolved fluorescence is used to measure the lifetime of the sample when the steady-state fluorescence spectra have changed and provides confirmation of the reason to this change. As the lifetime is the inverse sum of all decay rates of the excited state, the introduction of a quenching rate constant will immediately shorten the lifetime. A typical example of this effect is the decrease in lifetime due to energy transfer reactions.

### 3.5 Energy Transfer

An electronically excited molecule can return to its ground state by transferring its energy to a suitable acceptor molecule, in process called *Excitation Energy Transfer* (EET). This is a completely non-radiative process where the donor ( $D$ ) returns to its ground state while simultaneously exciting the acceptor ( $A$ ) according to



The process is usually dominated by two mechanisms. The *Dexter* mechanism requires orbital overlap between donor and acceptor and is governed by electron exchange interactions on very small distances.<sup>[59-60]</sup> The other mechanism, which is the only one considered in this thesis, is called *Förster energy transfer*. It is a long-range dipole-dipole interaction between the donor and the acceptor and is strongly distance and orientation dependent. It also requires overlap between the donor emission and acceptor absorption. As derived by Theodor Förster,<sup>[61-62]</sup> the rate of energy transfer,  $k_{EET}$ , can be determined by

$$k_{EET} = 8.79 \times 10^{-25} \frac{\phi_{f_D} \kappa^2}{\tau_D n^4 r_{DA}^6} \int_0^\infty I_F(\lambda) \varepsilon_A(\lambda) \lambda^4 d\lambda \quad (13)$$

In this equation,  $\phi_{f_D}$  and  $\tau_D$  are the unquenched fluorescence quantum yield and lifetime of the donor, respectively,  $r_{DA}$  is the distance in space between donor and acceptor and  $\kappa^2$  is the orientation factor between the transition dipole moments of the donor and acceptor.  $n$  is the refractive index of the solvent and the integral is the spectral overlap integral where  $I_F$  is the normalised fluorescence intensity of the donor and  $\varepsilon_A$  is the molar absorptivity of the acceptor.

The efficiency,  $E$ , of energy transfer, is often described together with the *critical Förster distance*,  $R_0$ , to show the strong distance dependence seen in equation 14.

$$E = \frac{R_0^6}{R_0^6 + r_{DA}^6} \quad (14)$$

$R_0$  is defined as the distance where the efficiency of EET is 50%. Using equation 13 combined with 14 an expression for  $R_0$  can be derived as

$$R_0^6 = 8.79 \times 10^{-25} \frac{\phi_{f_D} \kappa^2}{n^4} \int_0^\infty I_F(\lambda) \varepsilon_A(\lambda) \lambda^4 d\lambda \quad (15)$$



### 3.6 Photoisomerisation

---

Photochromic compounds which are the basis of this thesis are all molecules that undergo photoisomerisation. In this process a molecule ( $A$ ) changes structure without losing any atoms and is converted to a different isomer ( $B$ ), according to



The process is often but not always reversible where species  $B$  can be converted back to  $A$  by irradiation at another wavelength.  $A$  and  $B$  have different absorption spectra which often overlap at shorter wavelengths.

A measurement of photochromism efficiency is the final distribution of  $A$  and  $B$ , called the *photostationary distribution* (PSD), which is strongly wavelength dependent and can virtually be completely converted to form  $A$  or  $B$  if there is no absorption of form  $B$  or  $A$  respectively at the wavelength used for isomerisation.

Another measurement of photochromism efficiency is the quantum yield of photoisomerisation,  $\phi_i$ , defined as

$$\phi_i = \frac{\text{isomerised molecules}}{\text{photons absorbed}} = \frac{k_i}{k_i + k_f + k_{ic} + k_{isc} + k_Q} \quad (17)$$

and is derived from equation 7 where  $k_i$ , the rate of isomerisation, has been added as another pathway for the excited state molecule to be deactivated.

Due to the overlapping absorption of both isomers  $A$  and  $B$ , there are practical difficulties determining the quantum yield. If there is a wavelength where only one species absorbs, the quantum yield of photoisomerisation can be determined using a reference substance with known quantum yield,  $\phi_{iR}$ . By comparing the rate of absorbance change over time where only one of the species absorbs, the fitted rate constant,  $k_i$ , could be compared to the corresponding reference substance rate constant  $k_{iR}$  according to

$$\phi_i = \frac{k_i}{k_{iR}} \frac{\varepsilon_R}{\varepsilon} \phi_{iR} \quad (18)$$

where  $\varepsilon_R$  and  $\varepsilon$  are the molar absorption coefficients of reference and sample, respectively.

### 3.7 Molecular Complex Formation

---

A reaction in which a ligand,  $L$ , binds to a molecule,  $X$ , reversibly forming a complex  $L-X$  can be described as



and hence a binding constant,  $K$ , can be determined from the concentration of each species according to

$$K = \frac{[L-X]}{[L][X]} \quad (20)$$

To measure the binding constant, absorption with known molar absorptivity,  $\varepsilon$ , and fluorescence spectroscopy can be used. If the free ligand or the complex absorbs at a wavelength where no other species absorbs, the absorbance increase or decrease can easily be used to determine the binding constant as the absorbance change gives the concentration of all species. If that is not the case and the spectra overlap, a titration experiment can be made. Starting from a sample of  $X$ , the ligand is added in portions and the absorption or fluorescence change is observed until saturation occurs. The result is a series of spectra where known concentrations of ligand  $L$  are added to a concentration of molecule  $X$ . At every wavelength the total absorbance,  $A$ , is a linear combination of all the species, which by using Beer-Lambert law (4) gives

$$A = (\varepsilon_L[L] + \varepsilon_{L-X}[L-X] + \varepsilon_X[X])l \quad (21)$$

where  $\varepsilon_L$ ,  $\varepsilon_{L-X}$ , and  $\varepsilon_X$  are the molar absorption coefficients of ligand, complex and free molecule  $X$ , respectively. Both the concentrations and molar absorption coefficients may be unknown but the total concentration of ligand  $L$ ,  $[L_{tot}]$  is known,

$$[L_{tot}] = [L] + [L-X] \quad (22)$$

and the total concentration of molecule  $X$ ,  $[X_{tot}]$ , is known,

$$[X_{tot}] = [X] + [L-X] \quad (23)$$

Using these equations (22) and (23) together with the equilibrium expression (20) the concentration of each species can be expressed in  $X_{tot}$  and  $L_{tot}$ . As an example, the concentration of ligand  $L-X$  can be expressed as

$$[L-X] = \frac{\left([X_{tot}] + [L_{tot}] + \frac{1}{K}\right) - \sqrt{\left([X_{tot}] + [L_{tot}] + \frac{1}{K}\right)^2 + 4[X_{tot}][L_{tot}]}}{2} \quad (24)$$

By introducing the parameter  $\varepsilon_{\Delta L-X}$  that represents the difference in the overall absorption coefficient upon complex formation, the following expression can be used together with (24) for evaluation of UV/vis absorption titration data

$$\Delta A = \varepsilon_{\Delta L-X}[L-X] \quad (25)$$

where  $\Delta$  symbolises the change of absorbance and concentration before and after addition of  $X$ . As  $[L_{tot}]$  and  $[X_{tot}]$  are known throughout the titration, non-linear regression of the titration data at one or several wavelengths gives back  $\varepsilon_{\Delta L-X}$  and, most importantly, the binding constant  $K$ .

Furthermore, having the absorption spectra and the different concentrations as inputs, a *Singular Value Decomposition*-analysis (SVD) can be used together with a data-fitting program to deconvolute the overall spectra and resolve each separate spectrum of the different species.<sup>[63]</sup>

When binding sites on the molecule are independent and isolated, which is common to proteins or short DNA strands, the principle above is straightforward. However, large DNA strands are polymers with many binding sites which may or may not overlap with each other. Furthermore, if bound ligands interact with each other, the binding could be either cooperative or anti-cooperative. McGhee and von Hippel presented a method for calculating the fraction of bound ligands which take binding site size, cooperativity or anti-cooperativity into account.<sup>[64]</sup> In the model, DNA is considered as an infinite one-dimensional lattice of identical repeating residues, the DNA base-pairs. The relative amount of bound ligand to DNA is given by the binding density,  $\theta$ , defined as the concentration of bound ligand divided by the total concentration of base pairs. When a ligand binds, it occupies  $n$  base-pairs, which is referred to as the binding site size and made inaccessible for other ligands. In the non-cooperative case, the fraction of bound ligands,  $\theta$ , divided by ligands free in solution can be described by

$$\frac{\theta}{[L]} = K(1 - n\theta) \left( \frac{1 - n\theta}{1 - (n-1)\theta} \right)^{n-1} \quad (26)$$

and here the equilibrium constant  $K$  can be determined as well as the binding site coverage  $n$  using the above equations and analysis to determine the binding density and ligand concentration.



# 4 The Photochromic Molecules

This chapter gives an introduction to the results by explaining the photochromic compounds used in this thesis, their structure and properties. First, the spiropyran is presented, secondly the dithienylethene.

## 4.1 Spiropyrans

The common definition of spiropyrans is a 2*H*-pyran with the 2-carbon atom of the pyran group acting as a spiro atom connected to a second, often heterocyclic ring system as can be seen in Figure 4.1. Often the pyran is 2*H*-1-benzopyran, which has a second 6-ring system fused to the double bond next to the oxygen.

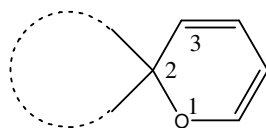
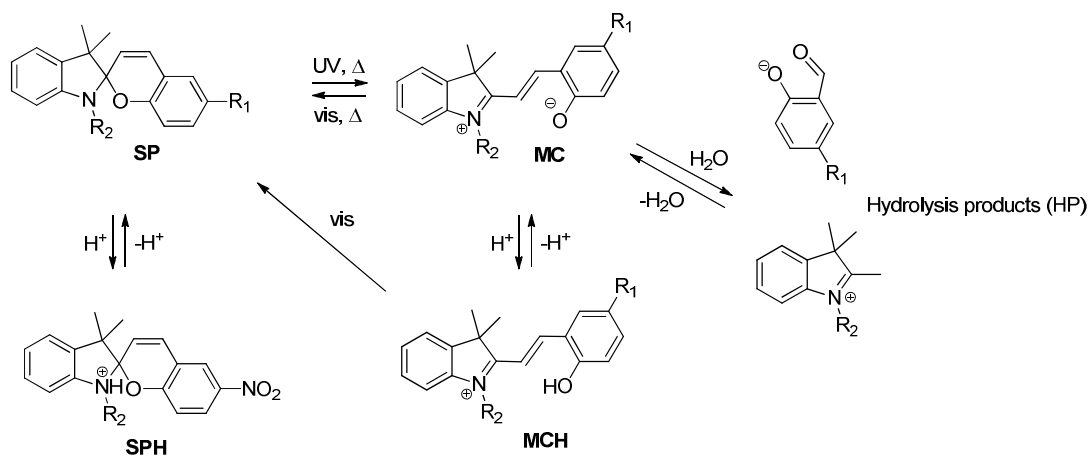


**Figure 4.1.** The definition of a spiropyran. The 2-carbon atom in the pyran group is connected to a second often heterocyclic ring system in a spiro manner.

This class of molecules is broad and opens up a large number of different compounds of which many have been prepared and their photochromic properties examined.<sup>[65-66]</sup> The photochromic reaction for this type of molecule is the cleavage of the ether bond to the spiro-2-carbon atom which breaks the spiro structure and instead gives a planar form named merocyanine (MC). The most stable MC has been proposed to be the *cis-trans*-isomerised planar structure seen in Scheme 4.1.<sup>[67]</sup>



**Scheme 4.1** The complete scheme of spiropyrans. The spiropyran (SP) can be isomerised either thermally or with UV light to form merocyanine (MC) which in water can be hydrolysed to the hydrolysis products (HP). Both SP and MC can be protonated to form the protonated spiropyran (SPH) as well as protonated merocyanine (MCH). MC and MCH can be isomerised back to SP using visible light.

Both SP and MC can be protonated at lower pH, then referred to as protonated spiropyran (SPH) and protonated merocyanine (MCH) respectively. In water, MC can be hydrolysed to form hydrolysis products (HP) something which is explained further in Paper IV.

In this thesis the spiropyran-merocyanine core structure has been used with modifications on either the nitrogen-tail marked  $R_2$  or on the phenol ring marked  $R_1$ . On  $R_2$ , either a chromophore has been attached (Paper II) to make an energy transfer couple or with addition of a positive charge (Paper III-VI) to (i) ensure water solubility and (ii) investigate the interaction of isomers with DNA. The most common substituent at the *para*-position of the phenola group ( $R_1$ ) is a nitro group, which was the first water-soluble spiropyran investigated in our lab.<sup>[51]</sup> The main purpose of this group is to stabilise the merocyanine form by electron with-drawing groups. Still, the substituent effect also influences the photostationary distribution, the  $pK_a$  of the phenol group as well as the thermal equilibrium between SP and MC.

There are a total of 9 different spiropyrans used in this thesis. They are presented in Table 4.1 with  $R_1$  and  $R_2$  substituents and numbered by order of appearance.

**Table 4.1** The numbered photochromic spiropyrans used in this thesis in order of appearance and with their difference substituents presented at  $R_1$  and  $R_2$ .

Name in Thesis	Used in Paper	$R_1$	$R_2$
1	II	$R_1 = -NO_2$	$R_2 = \text{---}CH_2CH_2CH_2C(=O)OH$
2	III, IV	$R_1 = -CN$	$R_2 = \text{---}CH_2CH_2CH_2N^+(CH_3)_2$
3	IV	$R_1 = -NO_2$	$R_2 = \text{---}CH_2CH_2CH_2N^+(CH_3)_2$
4	IV	$R_1 = -NO_2$	$R_2 = \text{---}CH_2CH_2CH_2NH^+$
5	IV	$R_1 = -NO_2$	$R_2 = \text{---}CH_2CH_2CH_2CH_2N^+(CH_3)_2$
6	IV	$R_1 = -NO_2$	$R_2 = \text{---}CH_2CH_2CH_2CH_2NH^+$
7	IV	$R_1 = \text{---}C(=O)H$	$R_2 = \text{---}CH_2CH_2CH_2N^+(CH_3)_2$
8	V, VI	$R_1 = \text{---}C(=NH_2^+)NH_2$	$R_2 = -CH_3$
9	V	$R_1 = \text{---}C(=NH_2^+)NH_2$	$R_2 = \text{---}CH_2CH_2CH_2N^+(CH_3)_2$

The spiropyrans can also be ordered by their substituents at positions  $R_1$  (columns) and  $R_2$  (rows) shown in Table 4.2. **1** is poorly water soluble while all other are water-soluble due to solubilising groups attached as  $R_1$  or  $R_2$ . Ways of making the spiropyran water-soluble have been made early<sup>[68]</sup> but it is not until recently that there have been more common examples.<sup>[69-74]</sup> All compounds except **1** have a positive charge at either  $R_1$  or  $R_2$ , **8** has its charge at  $R_1$  instead of  $R_2$ , and **9** carries a total of two positive charges.

**Table 4.2** The photochromic spiroopyrans used in this thesis organised based on their substituent at R<sub>1</sub> (columns) as well as R<sub>2</sub> (rows).

R <sub>2</sub>	R <sub>1</sub>	R <sub>1</sub> = -NO <sub>2</sub>	R <sub>1</sub> = -CN	R <sub>1</sub> = $\begin{array}{c} \text{O} \\ \parallel \\ \text{H} \end{array}$	R <sub>1</sub> = $\begin{array}{c} \text{NH}_2 \\ \parallel \\ \text{NH}_2^{\oplus} \end{array}$
R <sub>2</sub> = $\begin{array}{c} \text{OH} \\   \\ \text{C} \\   \\ \text{CH}_2\text{CH}_2\text{CH}_2\text{CH}_2 \end{array}$		<b>1</b>			
R <sub>2</sub> = -CH <sub>3</sub>					<b>8</b>
R <sub>2</sub> = $\begin{array}{c} \text{N}^{\oplus} \\   \\ \text{CH}_2\text{CH}_2\text{CH}_2\text{CH}_2 \end{array}$		<b>3</b>	<b>2</b>	<b>7</b>	<b>9</b>
R <sub>2</sub> = $\begin{array}{c} \text{NH}^{\oplus} \\   \\ \text{CH}_2\text{CH}_2\text{CH}_2\text{CH}_2 \end{array}$		<b>4</b>			
R <sub>2</sub> = $\begin{array}{c} \text{N}^{\oplus} \\   \\ \text{CH}_2\text{CH}_2\text{CH}_2\text{CH}_2\text{CH}_2\text{CH}_2 \end{array}$		<b>5</b>			
R <sub>2</sub> = $\begin{array}{c} \text{NH}^{\oplus} \\   \\ \text{CH}_2\text{CH}_2\text{CH}_2\text{CH}_2\text{CH}_2\text{CH}_2 \end{array}$		<b>6</b>			

In most organic solvents, the thermally isomer is SP and irradiation with UV light to form MC is far from efficient and reaches *ca* 60% MC. After irradiation, the compound is isomerised back to SP thermally or faster with visible light.

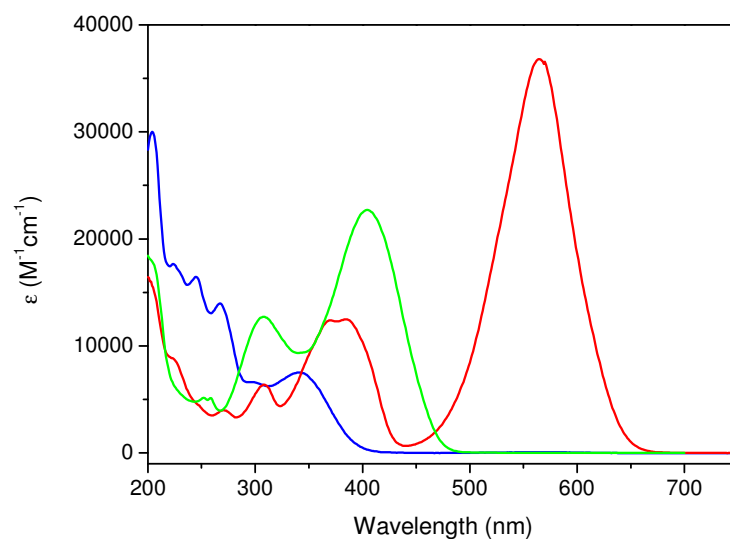


**Figure 4.2** Absorbance of **1** in acetonitrile. SP (blue), MC (red) and MCH (green).

The typical absorption of the SP, MC and the protonated MC (MCH) in acetonitrile can be seen in Figure 4.2 for **1**. SP absorbs only under 400 nm while the planar conformation of the open MC shifts the absorption to the visible region. The absorption maximum for MC is at 560 nm.

Upon acidification the phenolate group of MC is protonated which results in a hypsochromic shift of the spectrum to a maximum at 410 nm. This large

spectroscopic shift is explained by the loss of resonance of MC when the oxygen is protonated. As a consequence, the colour of the sample changes from pink/red to yellow. Furthermore, the thermal stability is dramatically increased in going from MC to MCH, something which has been used to create acid-induced opening of SP in organic solvents.

In water solution, SP, MC and MCH behave in a similar fashion but the thermal equilibrium is shifted towards MC. Left in dark, a ratio between SP and MC is established over time compared to virtually only SP in organic solvents. The zwitter-ionic properties of MC may explain this as the polar environment stabilises the dipole. The spectra of all species in water can be seen in Figure 4.3 where the molar absorption coefficient of a quaternary ammonium-tailed spiropyran **3** is presented.

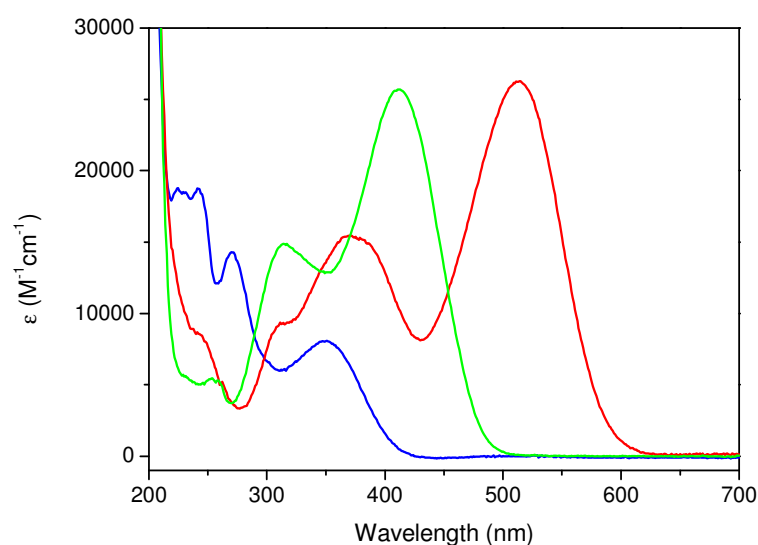


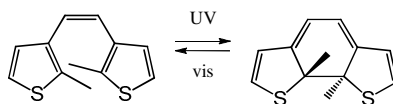
**Figure 4.3** Absorption spectra of **3** in water for SP (blue), MC (red) and MCH (green).

The large shift of the merocyanine absorption maximum from 560 nm towards 512 nm when moving from acetonitrile to water shows that the excitation energy is increased in the more polar environment. Usually, the excited state of a molecule has a larger dipole moment compared to the ground state and hence with increasing polarity, the  $S_1$ - $S_0$  gap is smaller resulting in an increase in the wavelength. Due to the zwitterionic properties of MC however, the solvent stabilises the ground state more than the excited state, and the absorption wavelength decreases.

## 4.2 Dithienylethenes

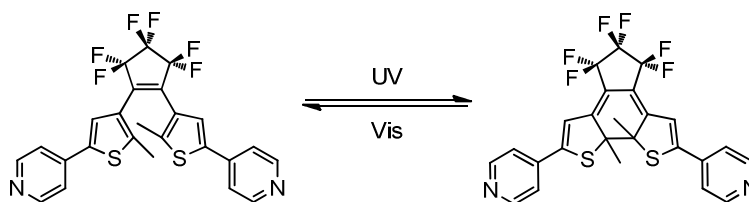
Dithienylethenes are photochromic compounds with very high fatigue resistance, *i.e.* resistance to photo-degradation.<sup>[75]</sup> Based on the knowledge of the stilbene photocyclisation reaction, the first type of dithienylethene was prepared in 1988.<sup>[76]</sup> The photochromic reaction is a  $6\pi$  photocyclisation which requires cyclisation to occur in a con-rotary manner (see Scheme 4.2) which results in methyl groups on the opposite sides of the newly formed bond, *i.e.* only the *R,R* and the *S,S* forms exist. Typically, the closed form is a racemic mixture of these two enantiomers.





**Scheme 4.2** The photochromic effect in dithienylethene. The stereochemistry may as well be the opposite direction of the methyl groups

The open form is closed by UV light which causes a bathochromic shift in the absorption as the closed form has a larger conjugated system. The thermally stable form is the open form but optimisation of the photochromism has resulted in extremely high thermal stability of the closed form. The DTE used in this thesis (Scheme 4.3) carries two pyridine groups attached to a dithienylperfluorocyclopentene.<sup>[77]</sup>



**Scheme 4.3** The dithienylethene derivative used in this thesis in its open form **DTEo** (left) and closed form **DTEc** (right).

In toluene the open form has an absorption spectrum in the UV region with an absorption maximum at 300 nm, see Figure 4.4. Irradiation of UV light ( $302\text{ nm}$ , ca  $1.5\text{ mWcm}^{-2}$ ) will within a minute convert the sample to closed isomer, a process which is very efficient with a quantum yield of ca 0.5, which is almost as much as possible due to the fact that it is only the anti-parallel form that can undergo ring closing. The photostationary distribution at this wavelength is virtually 100% conversion to the closed form.

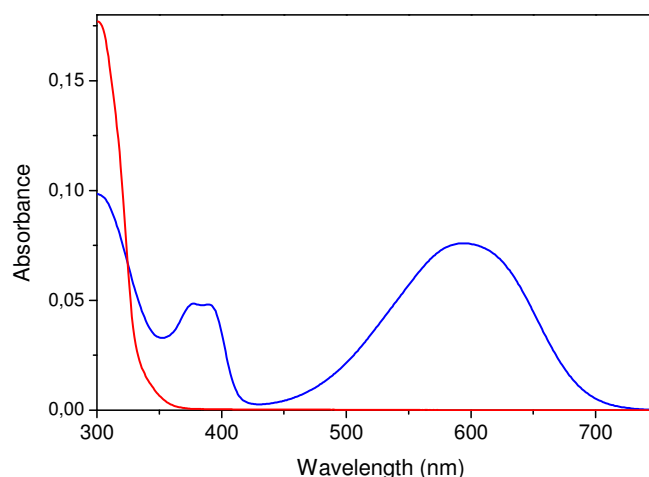


**Figure 4.4** Absorbance of **DTEc** (blue) and **DTEo** (red).

The closed form has two peaks in the absorption spectrum, one centred at 390 nm and one broad peak centred around 590 nm. By irradiation of light with a wavelength above 450 nm practically all the molecules return to the open isomer.

As both forms are extremely thermally stable and no photo-degradation can be seen after more than 10 cycles, this photochromic compound is a good candidate to perform logic operations as an almost fully binary response can be seen. As discussed in the next chapter, this molecule was used to mimic a molecular memory where it was shown to be the best candidate.

The water solubility of the DTE is negligible. However, by methylation of the pyridine nitrogens, which creates two permanent positive charges, it has been shown to be water soluble. In water, this modified DTE behaved the same with no large spectral differences. The DNA-binding of the modified DTE has also been investigated, which has shown that both forms bind the DNA-helix.<sup>[78]</sup>

---

## 5 Results

---

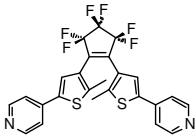
*This chapter summarises the results presented in the attached papers. To help the understanding, each paper starts with a table where all the photochromic compounds used in the paper are presented.*

### 5.1 Paper I – A Molecular Memory

---

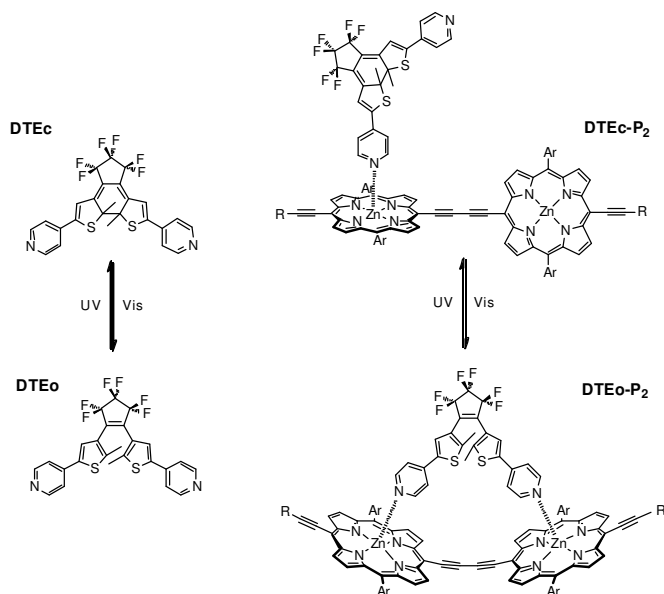
*A photochromic dithienylethene is coordinated to a porphyrin dimer in a light-controlled reversible way acting as a memory with non-destructive readout.*

**Table 5.1** Photochromic compound used in Paper I.

Name	Structure
<b>DTE</b>	

One of the most fundamental aspects of logic is to store information in such a way that if there are no inputs in a period of time, the state remains as it is, even after power loss, *i.e.* there is a resilience towards external non-input forces. Implementing this memory function with a molecule one needs to look for specific properties. There are at least four properties one should look for: The molecule should have (i) two different, optically distinguished forms, one of this state should represent a “1” and the other should represent a “0” which serves as the information you would like to store. (ii) An easy way of switching between these two forms, *i.e.* to write to the memory. Also, the forms must be (iii) thermally stable over time so that the memory remains at its state without losing information and finally (iv) the switching of these forms must not be degraded over time instead you should be able to rewrite to the memory multiple times. Addressing the first and second properties photochromic compounds are possible candidates as they have two forms, optically distinguishable as well as very easy switching between them using light. Addressing the two remaining properties, one needs to use very thermally- and photostable photochromic derivatives. As mentioned in the previous chapter, the photochromic dithienylethene derivative has been designed to conquer all these properties. The photochromic **DTE** (see Scheme 5.1) is very thermally stable and highly resistant to photo-degradation. Left in dark no isomerisation occurs over several weeks and it can hence be described as a simple memory by monitoring the absorbance of **DTEc** in the visible region as either 1 or 0. There is only one problem with **DTE** common to all photochromic molecules; they all are affected by the reading as we use light to read their state, the same light excites the molecule and may hence change its state. We call this, the *read of the memory is destructive over time*. To be able to make readout without affecting the distribution between the isomeric forms, we need to monitor the absorbance at a wavelength where the photochromic compound does not absorb. To conquer this problem, we used a porphyrin dimer which behaves differently depending on the state of **DTE** in the same solution.

The porphyrin dimer **P**<sub>2</sub>, see Scheme 5.1, has been previously studied in the context of electron transfer reactions. **P**<sub>2</sub> has been shown to be capable of coordinating Lewis bases such as pyridine.<sup>[79]</sup> Furthermore, the spectral properties are highly dependent on the conformation of the system.<sup>[80]</sup> As shown in Scheme 5.1, **DTEc** and **DTEo** are both capable of binding to the Zn centres of **P**<sub>2</sub> although the open form was shown to be able to coordinate to both atoms, to form a chelate, causing **P**<sub>2</sub> to planarise (*vide infra*).



**Scheme 5.1** Isomeric forms of the photochromic **DTE** and the **DTE-P**<sub>2</sub> complex (Ar = 3,5-di(octyloxy)phenyl, R = Si(C<sub>6</sub>H<sub>13</sub>)<sub>3</sub>)

The spectra of **DTEc**, **DTEo**, **P**<sub>2</sub> and the complexes **DTEc-P**<sub>2</sub> and **DTEo-P**<sub>2</sub> are shown in Figure 5.1. **DTEo** displays strong absorption at around 300 nm, **DTEc** absorbs up to 700 nm and **P**<sub>2</sub> has absorbance at even longer wavelengths. The possibility of pyridines to coordinate to the zinc centres stimulated us to study if the pyridine-appended DTE derivative may form structurally different complexes with **P**<sub>2</sub>, depending on its isomeric form. Indeed, when a sample of **DTEc** is added to **P**<sub>2</sub> a spectral change of the absorbance appears which has the same appearance as when pyridine is added (*vide infra*). Furthermore, irradiation of the sample using visible light above 450 nm, which isomerises the **DTEc** to **DTEo** causes a dramatic change of the spectrum. As can be seen in Figure 5.1, a large increase at 748 nm is observed. This spectral change can be explained by the coordination of **DTEo** to both zinc centres forming a chelate. **P**<sub>2</sub> is then locked in a more planar conformation which causes the absorbance increase at 748 nm. This observation is ascribed to the fact that **DTEc** is too rigid to coordinate to both zinc centres while **DTEo** is not.

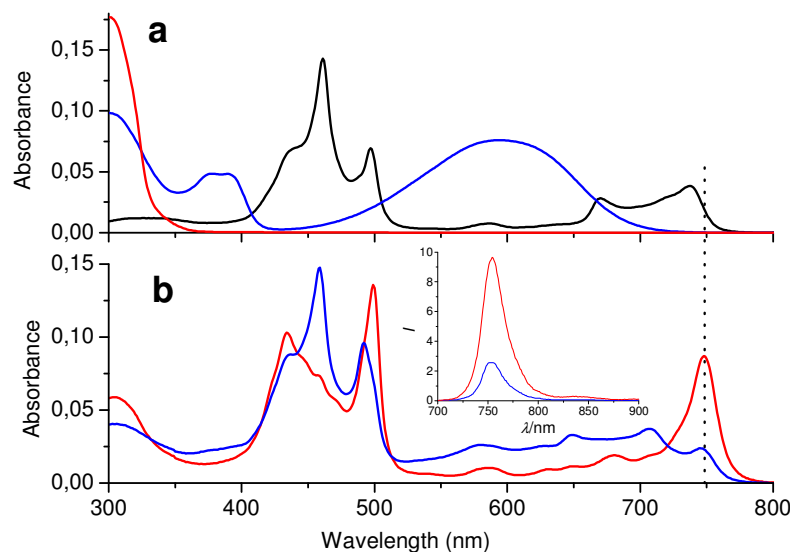


**Figure 5.1.** Absorption spectra in toluene of a) **DTEo** (red), **DTEc** (blue) and **P<sub>2</sub>** (black) and b) **DTEo-P<sub>2</sub>** (red) and **DTEc-P<sub>2</sub>** (blue). Inset: Emission spectra of **P<sub>2</sub>** in **DTEo-P<sub>2</sub>** (red) and **DTEc-P<sub>2</sub>** (blue) after excitation at 748 nm. It is clear that 748 nm light lies outside the absorption bands of **DTE** and that the overlap between **P<sub>2</sub>** emission and **DTE** absorption is negligible.

Since the absorbance at 748 nm is outside the region of the **DTE** absorption, it is possible to monitor which form **DTE** is in, without causing it to isomerise. The result solves all the four problems mentioned earlier and hence is an example of a molecular memory with non-destructive readout where the writing procedure is visible light irradiation and the erasing procedure is UV light irradiation. The reading is done at 748 nm. As also can be seen in the inset of Figure 5.1 the output does not necessarily have to be absorbance. By excitation at 748 nm fluorescence of **P<sub>2</sub>** can be seen. The variation of the fluorescence intensity upon isomerisation of the **DTE-P<sub>2</sub>** complex correlates well with the corresponding absorption changes at 748 nm.

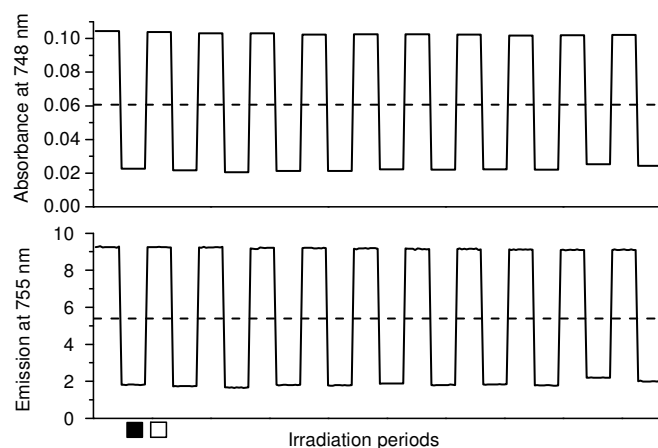
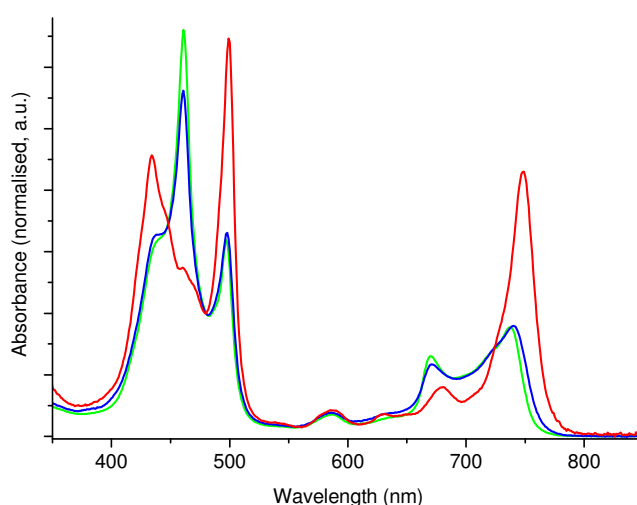


**Figure 5.2.** Photocycling of the **DTE-P<sub>2</sub>** complex in toluene. The absorbance at 748 nm (top panel) and emission intensity at 755 nm upon excitation at 748 nm (lower panel) measured for 5 s after each switching operation are shown: after UV irradiation for 30 s (■) and after broadband visible light irradiation for 18 min (□).

The photochromic reversibility of **DTE** is preserved in both complexes. Thus, we simulated a write-read-erase-read cycle for up to 10 times without observing any significant photo-degradation as can be seen in Figure 5.2. Keeping the sample in

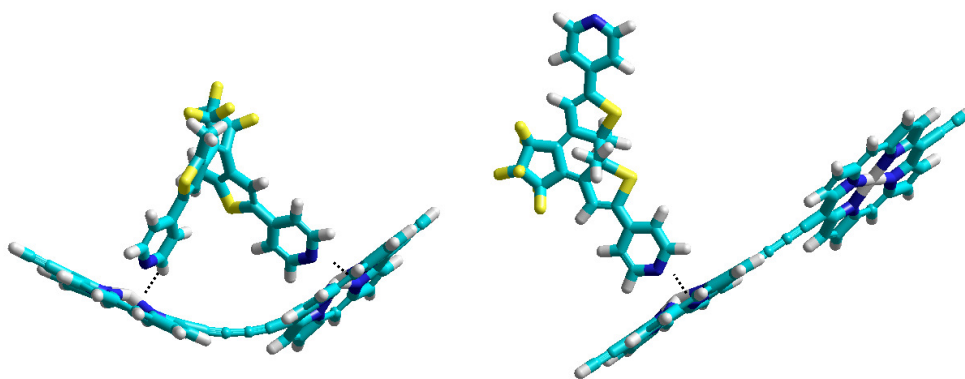
the dark caused no change in absorbance in weeks and continuous readout at 748 nm caused no significant decrease in the absorbance for 64 h which clearly shows that no interference with the isomeric state of **DTE** has occurred.

Further insight to the binding was gained by comparing spectra of **DTEc-P<sub>2</sub>** and **P<sub>2</sub>** with large excess of pyridine. As can be seen in Figure 5.3 where the ligand absorption has been subtracted, the spectra overlap well, which also confirms the binding of **DTEc** to only one of the zinc centres. This is in dramatic contrast to what is observed for **DTEo** where the absorbance at around 748 nm is increased substantially. The binding constant of **DTEc** to **P<sub>2</sub>** was determined to be  $2.0 \cdot 10^5 \text{ M}^{-1}$  and for the chelate **DTEo-P<sub>2</sub>** it was determined to be  $2.1 \cdot 10^6 \text{ M}^{-1}$ . The binding is hence approximately 10 times stronger for the chelated complex formed with **DTEo** compared to the complex formed with **DTEc**.



**Figure 5.3.** Absorption spectra in toluene of **P<sub>2</sub>** (*ca* 1  $\mu\text{M}$ ) together with large excess of pyridine (*ca* 10 mM, green), **DTEc** (*ca* 0.1 mM, blue), and **DTEo** (*ca* 15  $\mu\text{M}$ , red), respectively. The spectra are normalised at 480 nm, and the contribution from ligand absorption have been subtracted.

A molecular modelling (Figure 5.4) of the complexes using the Gaussian 03 program<sup>[45]</sup> suite was also carried out which confirms the planar (with respect to rotation between the porphyrins) form of **P<sub>2</sub>** when **DTEo** is forming the chelate.

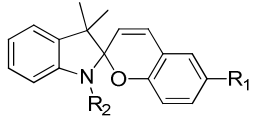
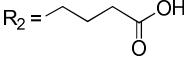
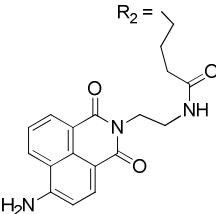
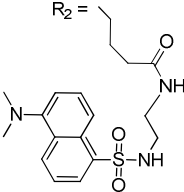
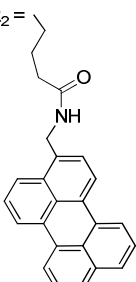


**Figure 5.4.** Geometry optimised structures of **DTEo-P<sub>2</sub>** (left) and **DTEc-P<sub>2</sub>** (right) complexes.

## 5.2 Paper II – A Reversible Sequential Logic Gate

Three spiropyran-fluorophore dyads are designed and presented as a sequential logic gate with base addition and red light irradiation as inputs.

**Table 5.2** Photochromic compounds used in Paper II. All are based on **1** with three different substituents at R<sub>2</sub>: 4-amino-1,8-naphthalimide (**1a**), dansyl (**1b**) and perylene (**1c**)

		R <sub>1</sub>	R <sub>2</sub>
<b>1</b>		R <sub>1</sub> = -NO <sub>2</sub>	
<b>1a</b>		R <sub>1</sub> = -NO <sub>2</sub>	
<b>1b</b>		R <sub>1</sub> = -NO <sub>2</sub>	
<b>1c</b>		R <sub>1</sub> = -NO <sub>2</sub>	

In logic devices it usually does not matter in what sequence an input is added to get an output. It does not matter if input 1 is first applied between input 1 and 2 in order for the output in an AND-gate to get activated. There is, as one may observe, no memory effect in the logic circuit. If input 1 is applied, the logic gate does not know if input 2 has been applied before or not, but if both are applied, the desired output is set. In complex logic circuits this can sometimes be a problem and hence when a memory effect is desired, these logic gates will not fulfil the task. Instead, one needs to add a memory effect to the logic gate such that the output is dependent on the order of the two inputs. This is called a *sequential* logic gate.

In this paper we focus on supramolecular dyad molecules which act as sequential logic gates with the photochromic spiropyran as the major part. The absorption difference between SP, MC and MCH is used to turn *on* or *off* quenching of a fluorophore appended at R<sub>2</sub> using excitation energy transfer based on the Förster

theory. Three different fluorophores (4-amino-1,8-naphthalimide, dansyl, and perylene) were carefully chosen to be attached to the spiropyran seen in Table 5.2 creating **1a**, **1b** and **1c**.

In organic solvents such as acetonitrile, used in this study, the spiropyran (SP) is the thermally stable species and virtually all of the merocyanine (MC) is thermally reverted to SP in minutes after being left in the dark. The absorption spectrum of all forms of **1** have been presented earlier (see Figure 4.2). With a UV lamp at 302 nm we reached a photostationary distribution of 61 % MC. By addition of trifluoroacetic acid (TFA) the protonated merocyanine (MCH) was formed, a process which was reversed by addition of the 1 equivalent phosphazene base (P<sub>2</sub>-Et).

The three fluorophore-residues on R<sub>2</sub> were chosen rationally from the recorded emission spectra which had overlap with both MC and MCH but no overlap with the absorption of SP. Based on the Förster theory of EET, fluorescence quenching due to energy transfer requires spectral overlap between the donor emission and acceptor absorption. We recorded the absorption of MC and MCH and looked for fluorophores with emission bands on the same wavelengths. Using equation 15 we could calculate the theoretical R<sub>0</sub>-value for MC-fluorophore pair as well as the MCH-fluorophore pair. The resulting R<sub>0</sub> values were in the range of 38-47 Å when MC was acceptor and 19-35 Å when MCH was acceptor. With a confirmation of non-existing overlap between SP absorbance and the emission of the fluorophores, the three different dyads were synthesised.

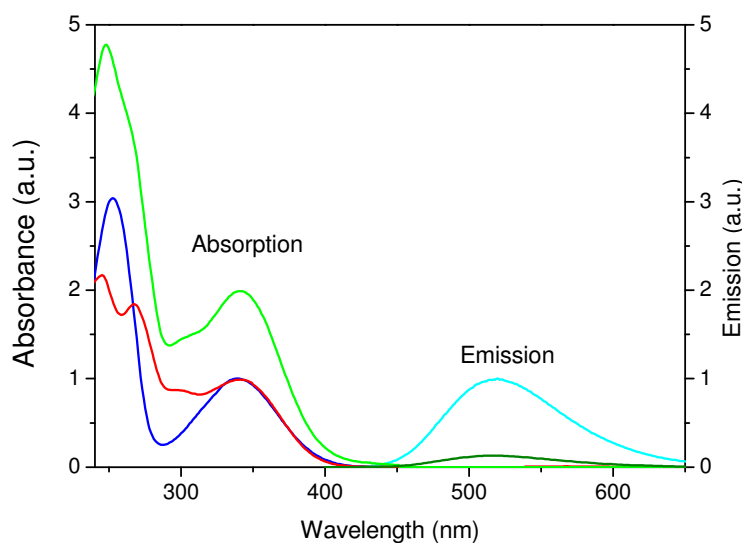


**Figure 5.5** Absorption of Dansyl (**b**) (blue), **1** (red) and **1b** (green) to the left. Emission of dansyl (**b**) (light-blue) and emission of **1b** (dark-green) to the right.

Absorption and emission spectra for one of the dyads (**1b**) and the reference substances SP and dansyl (**b**) can be seen in Figure 5.5. The absorption of the dyad **1b** was observed as equal to the combination of the two reference substances which indicates that the substances preserve their spectroscopic properties. A problem was observed by comparing the emission of the complex and the reference dansyl (**b**) alone. Even though the spectrum looks similar, a *ca* 90% quenching of the dansyl emission was observed when in the complex with SP. The quenching was assigned to electron transfer (ET) reactions as the redox energies are such that ET is thermodynamically favourable in all three dyads.



The expected *on-off* fluorescence quenching by conversion of the SP to MC was verified by UV light (302 nm). The quenching of **1b** was up to 44% which was clearly in the same range as the expected photostationary distribution between SP and MC determined to be of *ca* 45% MC. Similar quenching results (38% and 57%) were seen for the other dyads and hence we concluded that the energy transfer efficiency is virtually 100% in the MC form of the dyads. With an  $R_0$  of *ca* 40 Å and a distance between SP and fluorophore determined to be of maximum 15 Å this was also in well agreement with the observed fluorescence quenching due to EET.

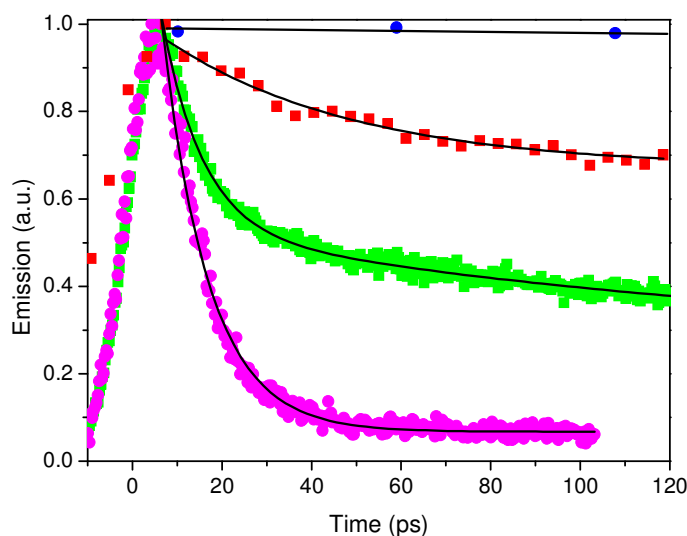


**Figure 5.6** Streak camera measurements of perylene (c) (blue), **1c-SP** (red), **1c-MC** (green) and **1c-MCH** (purple). The solid lines are only to guide the eye and do not correspond to the actual fit.

Using time-resolved fluorescence spectroscopy with a streak camera detector we derived the fluorescence lifetimes of the different forms of the dyads to confirm the observed steady-state results. Indeed, the lifetime was reduced from 926 ps (**1c-SP**) down to 8 ps (**1c-MC**) as seen in Figure 5.6, which is in well agreement with steady-state results.

The three dyads were realised as sequential logic gates with two inputs, addition of base, input 1, and irradiation with red light ( $\lambda > 430$  nm) as input 2. The initial state was chosen to be the protonated form of the merocyanine MCH. The output signal was chosen to be the fluorescence from the fluorophore with a high fluorescence as the *on* (1) state and quenched fluorescence as the *off* (0) state. In the initial state, the MCH absorption overlaps with the emission. This successfully quenches the fluorophore and the gate is in its *off* state. One can now choose to add the inputs in two sequential ways, either 1 followed by 2, or 2 followed by 1. In a sequential gate, only one of these two input combinations will give rise to an output signal.

By addition of base (input 1) to the initial state, the dyad is transferred to the MC form. With a good absorption overlap with the fluorophore, the emission remains quenched. However, in this state with absorption of the MC at 540 nm it will react to the red light (input 2) and easily transform to SP, where the fluorophore will be unquenched. Hence, applying input 2 will switch the fluorescence output to the *on* state.

If the input combination instead is started by red light, nothing happens due to the fact that MCH absorbs only below 500 nm. Hence, the system remains as it is after addition of input 2. Applying input 1, *i.e.* addition of base, causes MCH to revert to MC but still, no emission is increased as MC quenches the fluorescence. The only drawback to the system is the thermal instability of MC which causes the system to eventually return to SP after base is added. Still, in the appropriate time scale, the desired effect is sufficient. All the input combinations and their resulting emission are presented in Figure 5.7.

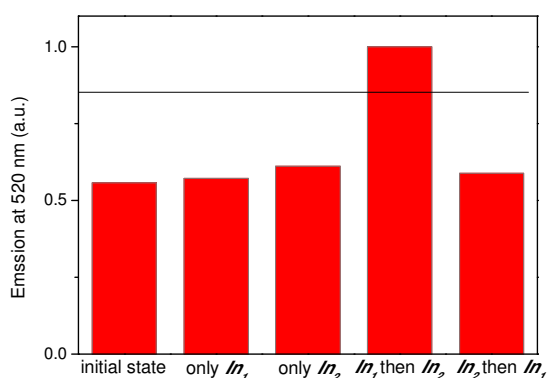


**Figure 5.7** Emission output for **1b** of the logic device after all input combinations.

The sequential logic gate could be repeated up to 5 cycles using TFA and UV light to reset SP to the MCH as seen in Figure 5.8.

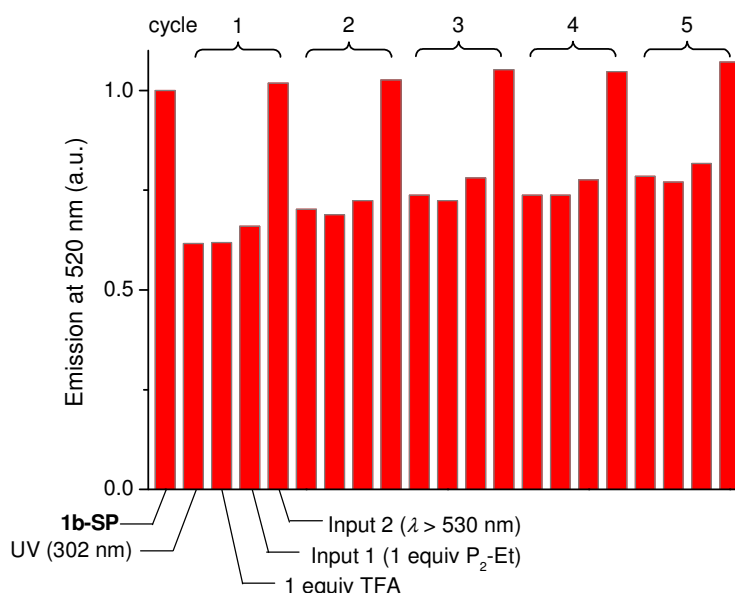


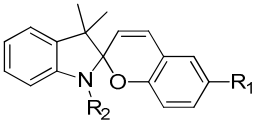
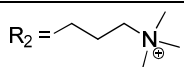
**Figure 5.8** Repeated sequential logic results performed in total of 5 cycles for **1b**

As a last touch to the logic gate, an anthracene derivative was used to achieve reversible logic, *i.e.* unambiguous mapping of input vectors to output vectors.

### 5.3 Paper III – DNA-Binding as a Logic AND-Gate

A cyano-substituted spiropyran is realised as a logic AND-gate with binding to DNA as output and low pH and UV light as inputs.

Table 5.3 Photochromic compound used in Paper III.

	R <sub>1</sub>	R <sub>2</sub>
<b>2</b>	R <sub>1</sub> = -CN	R <sub>2</sub> = 

The photochromic family of spiropyrans undergoes dramatic geometric changes upon isomerisation from the bulky SP isomer to the planar MC isomer. The interaction of these forms with DNA, the fundamental building block of life and crucial in all cells, was investigated based on previous observations of binding of MC.<sup>[51]</sup>

In this paper we observed that the structural changes the photoswitch undergoes, allows it bind to DNA only in the protonated merocyanine form, MCH, which requires the input of UV irradiation and acidification. This can be seen as a biological AND gate, where UV-light and protons are to be regarded as inputs. The usually more acidic conditions observed in and around a cancer cell<sup>[31-32]</sup> can serve as an internally controlled input, or a “sensing” input. The UV light irradiation then serves as an externally controlled input with the possibility to expose only the part of the body where the cancer cells are located. The potential cell death due to strong DNA-binding may therefore be obtained with high selectivity toward cancer cells, creating a cytotoxin which acts binary according to the conditions of its surroundings.

In aqueous solution at pH 7, a thermal equilibrium is established with a 90/10 composition of SP/MC. Under UV exposure, 254 nm, a photostationary distribution (PSD) is reached at a ratio 65/35 SP/MC. Acidification of MC causes it to protonate ( $pK_a = 4.5$ ). Spectra of SP, MC and MCH can be seen in Figure 5.9.

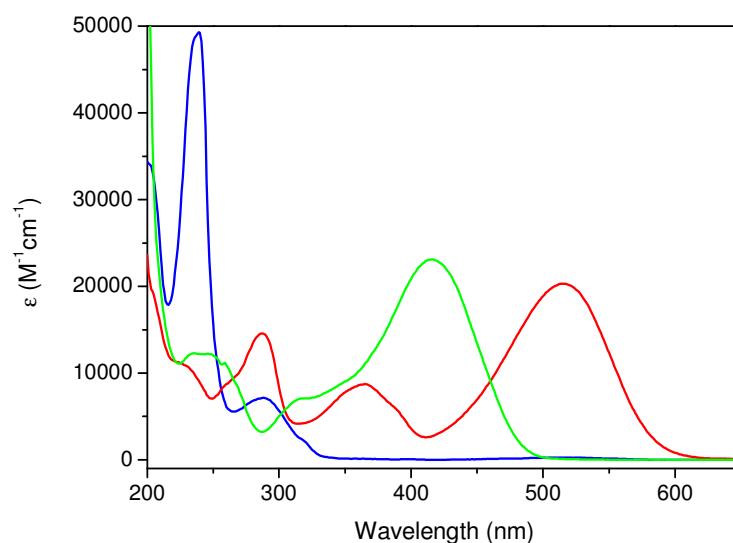


**Figure 5.9.** Absorption spectra of SP (blue), MC (red) and MCH (green) of the Cyano-substituted spiropyran (**2**).

By the addition of DNA to a sample of spiropyran in its different forms and measuring the absorption spectra, interaction with the DNA can be investigated. Four different samples were prepared: SP at pH 7 and pH 6 (no UV, Figure 5.10 a and c respectively), and two samples irradiated by 254 nm UV light for ca 50 s at pH 7 and at pH 6 (UV, Figure 5.10 b and d).

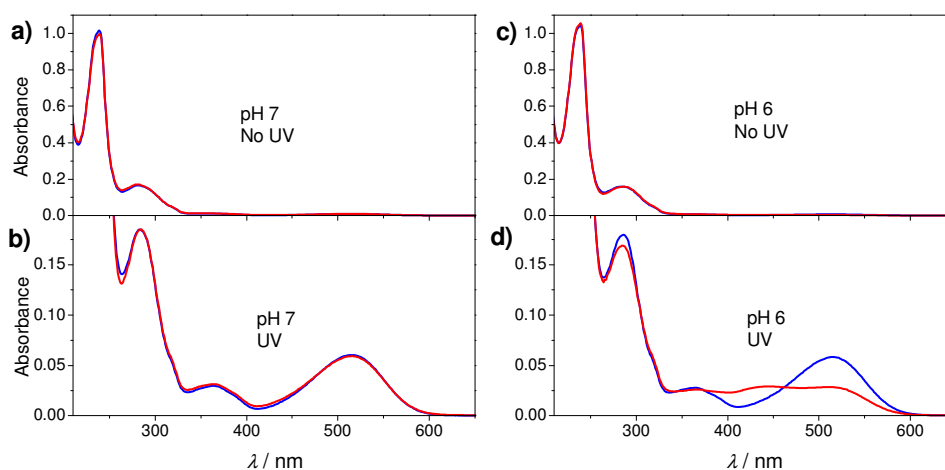


**Figure 5.10.** Absorption spectra of **2** in the absence (blue) and in the presence (red) of ct-DNA at pH 7 (a and b) and at pH 6 (c and d). In b and d, the samples were exposed to ca 50 s UV light to stimulate the light induced isomerisation **2SP**→**2MC** to a final 90/10 distribution **2SP/2MC+2MCH**. In d, it is clearly seen that the spectral changes upon addition of DNA are dramatic at pH 6 after UV irradiation, while no or only minor changes are observed for all other combinations of pH and UV dose. The contributions from DNA absorption have been subtracted for ease of comparison. The concentration of **2** and DNA was ca 20 μM and 110 μM, respectively, and the NaCl concentration of the solutions were 10 mM. Note that different y-axis scales have been used for the top and the bottom rows in order to better visualise the effect of DNA on the absorption spectra of the open forms **2MC** and **2MCH** which were not formed in the absence of UV exposure (a and b).

The spectra with and without DNA are almost completely super-imposable in all cases except after UV irradiation at pH 6 where a *ca* 50% decrease in absorbance at 516 nm together with an increase at 440 nm is observed. Using linear dichroism where DNA is oriented in a macroscopic flow and ligands hence will be oriented as well, we observed a new peak at 440 nm, which corresponds very well to the absorbance at 440 nm observed in the absorption spectroscopy measurements (Figure 5.11).

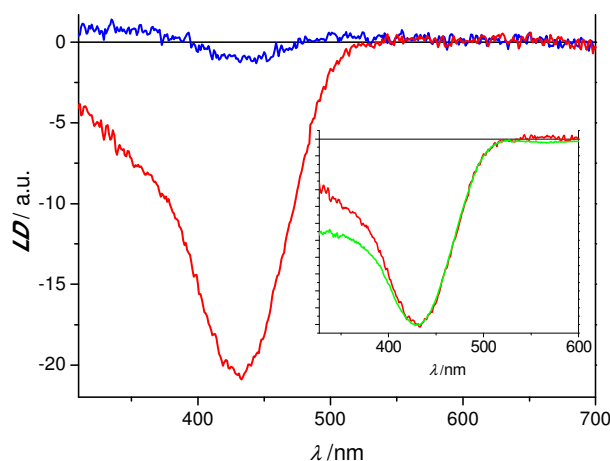


**Figure 5.11.** Flow oriented LD spectra on samples of **2** and ct-DNA after 10 min UV irradiation at pH 7 (blue) and at pH 6 (red). The amplitude of the LD signal is *ca* 20 times higher at pH 6 compared to pH 7. The inset shows the good agreement between the LD spectrum at pH 6 (red) and the absorption spectrum of DNA-bound **2MCH** (green). The negative absorption spectrum is shown for ease of comparison. The concentration of **2** and DNA was *ca* 50  $\mu$ M and 90  $\mu$ M, respectively, and the NaCl concentration of the solutions was 10 mM.

Using the absorbance decrease at 516 nm the microscopic binding constant of **2MCH** was determined to be  $2.9 \cdot 10^5 \text{ M}^{-1}$ . However, seeing all three forms as binding agents, a macroscopic binding constant can be determined which is dependent on the amount of UV irradiation and pH. Thus, seeing UV irradiation and the lowering of pH from 7 to 6 as binary inputs, a truth table with the binding as output can be established (Table 5.4). This can be interpreted as an AND-gate as both inputs UV light and acidification are required. Hence, this is an example of a biological binary device where the desired output (DNA-binding), is achieved after an externally controlled input (UV-irradiation) as well as an internally “sensing” input (pH). From the LD spectrum and the absorbance measurements the  $LD^f$  was calculated and a binding angle established to  $76 \pm 5^\circ$  which indicates that **2MCH** is intercalating between the bases in the DNA-helix.

**Table 5.4** Truth table for the AND logic gate using UV light and H<sup>+</sup> as inputs and the macroscopic DNA-binding constant of **2** as output.

Input		Output
UV <sup>[a]</sup>	H <sup>+</sup> <sup>[b]</sup>	<i>K</i> [M <sup>-1</sup> ]
0	0	<5 (low)
0	1	<5 (low)
1	0	18 (low)
1	1	455 (high)

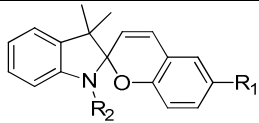
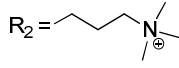
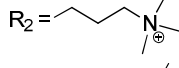
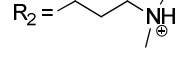
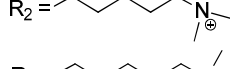
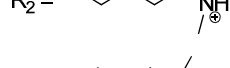
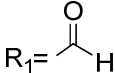
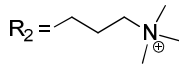
[a] 0 = no UV; 1 = 50 s UV exposure.

[b] 0 = pH 7; 1 = pH 6

## 5.4 Paper IV – Spiroprans in Aqueous Solution

The thermal and photoinduced isomerisation processes for six water-soluble spiropyrans are investigated between pH 0 and pH 10. The hydrolysis reaction is also investigated by experimental and theoretical means.

**Table 5.5** Photochromic compounds used in Paper IV.

	R <sub>1</sub>	R <sub>2</sub>
<b>2</b>	R <sub>1</sub> = -CN	R <sub>2</sub> = 
<b>3</b>	R <sub>1</sub> = -NO <sub>2</sub>	R <sub>2</sub> = 
<b>4</b>	R <sub>1</sub> = -NO <sub>2</sub>	R <sub>2</sub> = 
<b>5</b>	R <sub>1</sub> = -NO <sub>2</sub>	R <sub>2</sub> = 
<b>6</b>	R <sub>1</sub> = -NO <sub>2</sub>	R <sub>2</sub> = 
<b>7</b>	R <sub>1</sub> = 	R <sub>2</sub> = 

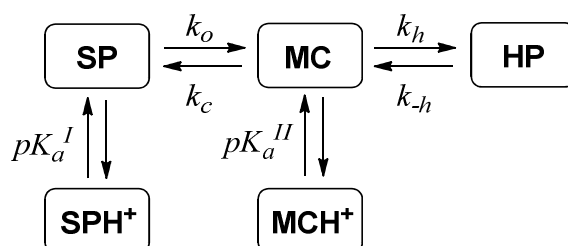
In Paper III we optimised the *pK<sub>a</sub>*-value of the merocyanine form of spiropyran **2** to get a sufficient concentration of the protonated form available for binding in the low pH regime (pH 6) compared to pH 7. Hence, we had a large number of spiropyrans synthesised for water solutions in our lab, which opened up the possibility to characterise similarities and differences of the behaviour in aqueous environment.

As an aim to get better DNA-binding candidates of the spiropyran, we started to focus on these properties and made a comparison study of all water-soluble spiropyran derivatives. Initially, the effect of the substitution pattern (R<sub>1</sub> and R<sub>2</sub>) on

the rate of hydrolysis was investigated, but the study was soon expanded to a full characterisation of all derivatives (2-7) shown in Table 5.5 over a broad pH range.

At very low pH ( $\text{pH} < 1$ ) we observed a spectroscopic change of the SP isomer. This new species was observed to be non-photochromic and was suggested by Wojtyk *et. al.*<sup>[81]</sup> to be the protonated spiropyran (SPH). Together with the protonated merocyanine (MCH) there are in the pH 0-10 interval up to four different species available in solution. The claimed SPH molecule is subject to debate as Biczok assigned the same species to be the *cis*-MCH<sup>[82-83]</sup> compared to the “normal” *trans*-MCH. We made efforts to determine this using NMR but the results were inconclusive. However, as the protonated species is thermally stable over months, we find it very unlikely to be the *cis*-MCH conformer which is expected to isomerise much faster to the *trans*-MCH form.

The hydrolysis of the MC species at around neutral pH was observed, something which has been suggested to be a big drawback of the spiropyran in aqueous solution.<sup>[69]</sup> Hence, studies of all the derivatives at different pH was started which generated a model of all species together with the explanation of our observations of hydrolysis based on both experimental data as well as computational studies. The full model is seen in Scheme 5.2 where the thermal rate constants are presented as well as the different acidity constants, which are presented in Table 5.6. We focused on the thermal process as there are other examples of characterisation of the dynamics of the spiropyran-merocyanine photoisomerisation.<sup>[84]</sup>



**Scheme 5.2** A complete model of all species in solution for the spiropyrans in water with rate constants and acidity constants defined.

**Table 5.6**  $pK_a$ -values of SPH ( $pK_a^I$ ) and MCH ( $pK_a^{II}$ ) for 2-7.

	2	3	4	5	6	7
$pK_a^I$	0.4	0.4	0.4	1.6	1.4	0.4
$pK_a^{II}$	4.4	3.7	4.2	4.4	4.2	4.5

At pH 6 to 8, the SP is thermally opened to MC which in turn is hydrolysed. The hydrolysis is a retro-aldol reaction, which generates two synthetic reactants used to make the spiropyran. Following the addition of SP in buffered aqueous solution there is a growing peak belonging to MC around 500 nm which starts from zero absorbance and increases (MC is formed from SP). After a peak increase in the timescale of hours, the peak starts to decrease together with the formation at shorter wavelengths of the absorbance of the hydrolysis products (HP). The spectrum at

pH 7 after 12 000 min for **3** can be seen in Figure 5.12. The residual absorbance of MC at equilibrium clearly shows that the hydrolysis reaction is reversible.

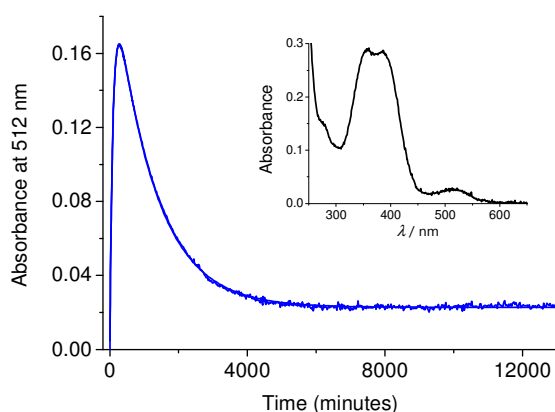


**Figure 5.12** Absorbance changes at 512 nm for **3** after the addition of SP to water at pH 7.0. An increase at 512 nm showing the formation of MC is followed by a decrease of absorbance when MC is hydrolysed. The inset is the absorbance end spectrum at 12 000 min showing the absorbance of the hydrolysis products (HP) as well as a clear absorbance of MC left in solution.

As only MC absorbs above 500 nm and no protonated species are available at pH 7, the model in Scheme 5.2 in this pH range could be simplified to



By observing the absorbance change of MC, the derived rate constants could be determined using a Laplace transform analytical solution<sup>[85]</sup> and the values are shown in Table 5.7 for all compounds in the study (2-7).

**Table 5.7** Rate constants for the thermal processes, of compounds 2-7 at 25 °C at pH 7.

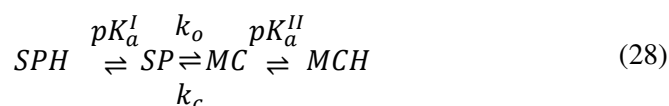
	$k_o$ [min <sup>-1</sup> ]	$k_c$ [min <sup>-1</sup> ]	$k_h$ [min <sup>-1</sup> ]	$k_{-h}$ [min <sup>-1</sup> ]	$k_o/k_c$
<b>2</b>	$5.6 \times 10^{-3}$	$3.4 \times 10^{-2}$	$2.6 \times 10^{-3}$	$5.4 \times 10^{-5}$	0.16
<b>3</b>	$3.5 \times 10^{-3}$	$5.1 \times 10^{-3}$	$2.2 \times 10^{-3}$	$9.8 \times 10^{-5}$	0.69
<b>4</b>	$3.4 \times 10^{-3}$	$3.9 \times 10^{-3}$	$1.8 \times 10^{-3}$	~0	0.87
<b>5</b>	$5.2 \times 10^{-3}$	$1.4 \times 10^{-3}$	$6.5 \times 10^{-4}$	$1.9 \times 10^{-5}$	3.7
<b>6</b>	$4.4 \times 10^{-3}$	$1.5 \times 10^{-3}$	$6.1 \times 10^{-4}$	$1.1 \times 10^{-5}$	2.9
<b>7</b>	$2.1 \times 10^{-2}$	$5.0 \times 10^{-2}$	$2.0 \times 10^{-3}$	$1.2 \times 10^{-4}$	0.42

The pH effects of SP→MC formation, MC hydrolysis, and SP/SPH concentration were investigated over a large pH interval (pH 0 to pH 10) for the compounds with different substituents on the phenol group (R<sub>1</sub>). Hence, we concentrated on **2**, **3**,



and **7** in this section. These compounds have groups at R<sub>1</sub>, which have been shown to control the  $pK_a$  of MCH.<sup>[86]</sup> The kinetic model in equation 27 was also used at pH 6 to pH 10. No significant changes in the rate constants were observed compared to pH 7, except from the hydrolysis reaction, which experienced a slight increase between pH 9 and pH 10. This indicates that the nucleophilic attack on the MC to cause hydrolysis most likely is the water molecule instead of OH<sup>-</sup>, at least at pH below 10.

At low pH (0-1) we observed the formation of SPH when dissolving SP in the buffered solutions. In this situation, with a  $pK_a$  around 4 for MCH (see Table 5.6), the most stable species is MCH and indeed, the absorbance was observed to slowly increase around 400 nm where MCH absorbs. However, as SPH cannot be directly converted to the open merocyanine form without first being deprotonated to SP, the observed rate of MCH formation is extremely slow. In this situation, the acid-base reactions are extremely fast compared to the SP-MC conversion. The following kinetic model was applied:



However, the [MC]/[MCH] equilibrium is shifted to virtually 100 % MCH. Hence, the kinetic situation is reduced to a model which includes only SPH, SP, and MCH:



The growth of MCH absorbance could be fitted to a mono-exponential rate expression. If we assume that all MC is instantly protonated to MCH and SP is in constant fast equilibrium between SPH and SP, the rate of opening of SP could be derived from the fitted exponential corrected by the equilibrium between SP and SPH according to

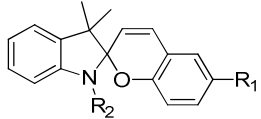
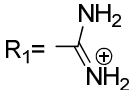
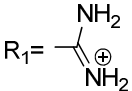
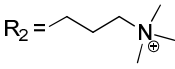
$$k_{obs} = \frac{[SP]}{[SP] + [SPH]} k_o \quad (30)$$

where  $k_{obs}$  is the fitted mono-exponential rate constant. The values of  $k_o$  at pH 0 and 1 were calculated to be  $5.0 \times 10^{-3} \text{ min}^{-1}$  and  $5.3 \times 10^{-3} \text{ min}^{-1}$  for **2**,  $4.0 \times 10^{-3} \text{ min}^{-1}$  and  $3.4 \times 10^{-3} \text{ min}^{-1}$  for **3** and  $1.3 \times 10^{-2} \text{ min}^{-1}$  and  $2.0 \times 10^{-2} \text{ min}^{-1}$  for **7**. These values agree well with the corresponding values at pH 5 to pH 10. A similar analysis between pH 2 and pH 4 gave unchanged rate constants. This showed that the thermal rate constants are constant over the whole pH interval 0-10. Hence, no accelerated acid-induced opening could be seen, rather all formed MCH by addition of acid is due to the concentration shift towards MCH when MC is formed from SP. The observation of no hydrolysis at this low pH also indicates that most likely, MCH is not susceptible to hydrolysis. This notion was further supported by computational means.

## 5.5 Paper V – DNA-Binding of Amidine Spiropyrans

Two amidine-substituted spiropyrans are shown to interact with DNA in a pH-dependent 4-state-model where both merocyanine and protonated merocyanine bind to DNA.

**Table 5.8** Photochromic compounds used in Paper V.

		$R_1$	$R_2$
<b>8</b>			$R_2 = -CH_3$
<b>9</b>			

Inspired by the DNA binding results in Paper III the interaction of the merocyanine to DNA was characterised even further. Amidine groups such as the one in Table 5.8 are present in well-known DNA-binders.<sup>[87-88]</sup> The first synthesised amidine spiropyran was **8** which had no ammonium tail attached to the indoline nitrogen ( $R_2$ ). How the DNA-binding depends on number of charge and position of the charges together with tail or no-tail at  $R_2$  were the questions we tried to answer in this study. As a reference amidine spiropyran, **9** was synthesised carrying two permanent charges, one from the amidine group and one from the ammonium tail at  $R_2$  found on the rest of the spiropyrans. **8** was observed to have the highest [MC]/[SP]-ratio at thermal equilibrium in water of all studied spiropyrans, up to 82% MC, and still have a comparably low hydrolysis rate,  $3.4 \times 10^{-4} \text{ min}^{-1}$  at pH 7.0. **9** instead is more similar to the rest of the spiropyran compounds with a ratio of MC up to 15% and a hydrolysis rate at pH 7 of  $1.7 \times 10^{-4} \text{ min}^{-1}$ . Absorption spectra of **8** and **9** can be seen in Figure 5.13.

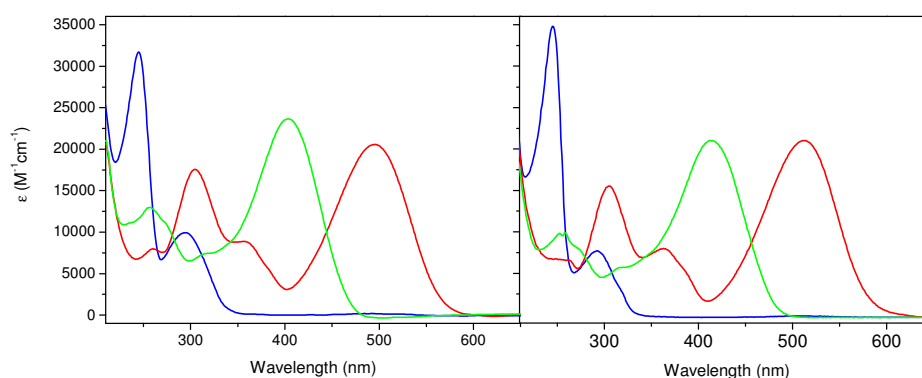


**Figure 5.13** Absorption spectra of SP (blue), MC (red) and MCH (green) for **8** (left) and **9** (right).

Based on our previous knowledge of DNA-binding, SP show no or very little interaction with DNA, and, the bound species was found to be MCH and not MC. What would happen if we increase the number of positive charges? Most likely, the binding will be enhanced in the protonated form, but will it be enough to see binding of SP?

The spectra of SP with and without DNA for **8** and **9** are seen in Figure 5.14. With a large concentration DNA added, we see no or very small signs of DNA interaction. **8** shows no interaction while **9** shows very small effects, most likely due to electrostatic interactions. Titration of DNA was hard to perform due to the overlapping DNA absorbance and the very small spectroscopic change.

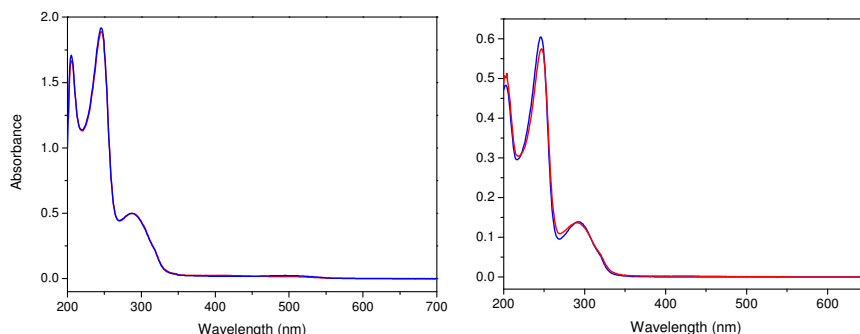


**Figure 5.14** Absorption spectra of SP with (red) and without (blue) DNA for **8** (left) and **9** (right),

To gain more knowledge of the DNA binding character, UV/vis absorption titrations were performed with salmon-sperm DNA for MC and MCH. Due to the pH effects seen previously in Paper III, titrations were made at pH 5, 6, 7, 8 and 9. This is the interval where the DNA B-helix is stable.<sup>[89-93]</sup> The results of **8** are seen in Figure 5.15.

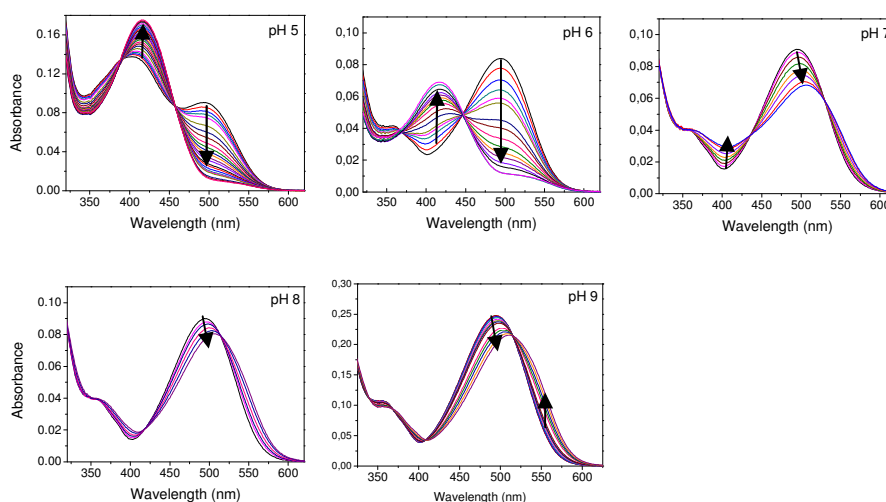


**Figure 5.15** DNA titration of **8** MC/MCH from top-left to bottom right at pH 5, 6, 7, 8 and 9.

At low pH the initial spectrum is dominated by the MCH species. After addition of DNA the absorbance of MCH is red-shifted and increased and the remaining MC is decreased. At higher pH, this effect is replaced by a red-shift and decrease of MC absorbance instead. Interestingly, this effect is large for **8** but as seen in Figure 5.16 a similar effect is much smaller for **9** where the charge is increased and the indoline nitrogen bears a positively charged amino tail.

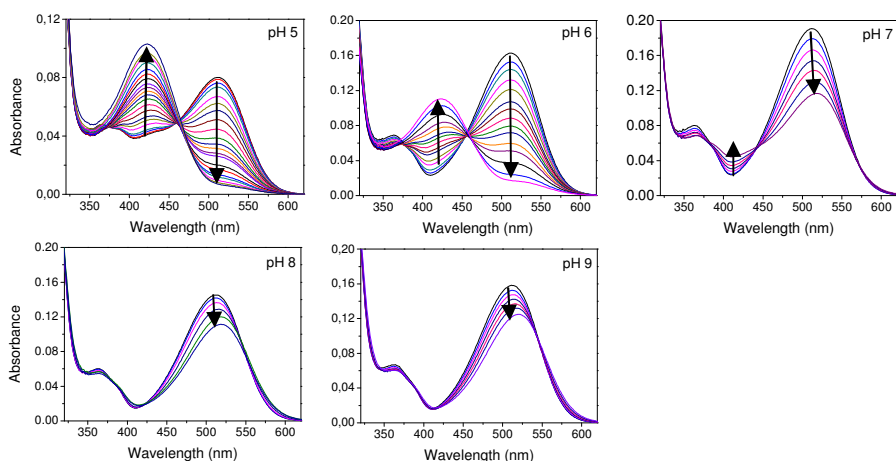
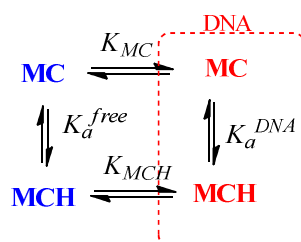


**Figure 5.16** DNA titration of **9** MC/MCH from top-left to bottom right at pH 5, 6, 7, 8 and 9.

These results indicate a binding of both MC and MCH. Inspired by this pH dependent binding, we suggested a model which would explain the results. Presented in Scheme 5.3, we have competitive binding of both MC and MCH and most likely a separate  $pK_a^{DNA}$ .



**Scheme 5.3** The proposed 4-state model of DNA-binding of MC and MCH dependent on both the acidic constants at DNA as well as two separate binding constants.

With this model, we used the following steps to derive all binding and acidic constants: (i) The  $pK_a^{free}$  was separately determined to be 4.5 and 4.1 for **8** and **9** respectively. (ii) At pH 9 we assume no presence of MCH and fit the titration data to a model with only MC free in solution and MC bound to DNA and determined a binding constant for MC ( $K_{MC}$ ). In this titration, the end spectrum of MC with DNA could be calculated representing the spectrum of MC bound to DNA. (iii) Titration at pH 5 was fitted to a model and used to calculate the end spectrum, consisting only of MCH bound to DNA using the same assumption as for MC before. (iv) The two calculated end spectra were used to fit the titration spectra at pH 6, 7 and 8 and derive the end concentration of bound MCH and MC at each pH. The calculated spectra can be seen in Figure 5.17.

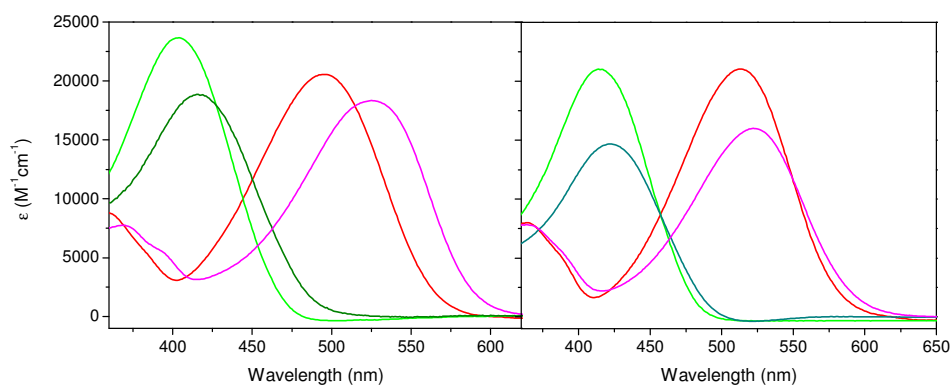


**Figure 5.17** Absorption spectra of MCH free (light green), MCH bound to DNA (dark green), MC free (red) and bound to DNA (purple) for **8** (left) and **9** (right).

With these values, a pH dependent ratio of MC and MCH bound to DNA could be fitted to a model and  $pK_a^{DNA}$  could be determined. (v) With all other constants known, the binding constant of MCH was determined following the equation

$$\frac{K_{MC}}{K_{MCH}} = 10^{pK_a^{free} - pK_a^{DNA}} \quad (31)$$

As a compliment to the study theoretical binding isotherm based on the McGhee and von Hippel method was globally fitted to all the titrations with the use of singular value decomposition (SVD) of the data. With a good fit with binding site coverage of 2 per base-pair, these results were in agreement with the previous ones. The results are summarised in Table 5.9.

**Table 5.9** Binding constants and acidic constants as well as the ratio of bound species for **8** and **9**. In parenthesis is the fitting to the non-cooperative McGhee-von Hippel model with the nearest neighbor exclusion ( $n = 2$ ).

	<b>8</b>	<b>9</b>
$pK_a^{free}$	4.5	4.1
$pK_a^{DNA}$	6.7 (6.4)	6.6 (6.5)
$K_{MC} (M^{-1})$	$9.9 \cdot 10^2 (1.3 \cdot 10^3)$	$4.3 \cdot 10^3 (2.2 \cdot 10^3)$
$K_{MCH} (M^{-1})$	$1.6 \cdot 10^5 (1.2 \cdot 10^5)$	$1.4 \cdot 10^6 (6.1 \cdot 10^5)$
Bound ratio at pH 6 (% MCH / % MC)	99/1	99/1
Bound ratio at pH 7 (% MCH / % MC)	34/66	28/72
Bound ratio at pH 8 (% MCH / % MC)	8/92	4/96

DNA-binding was confirmed using LD spectroscopy (Figure 5.18) where a large peak at 440 nm could be seen at lower pH (pH 6) whereas a peak above 500 nm was seen at pH 8.0 corresponding well with the calculated end spectra of MC and MCH in DNA for both species.

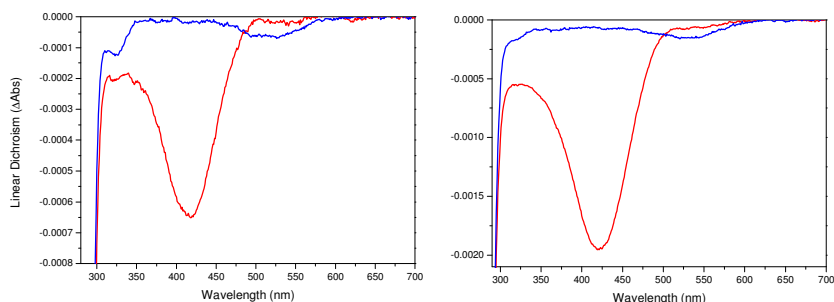


**Figure 5.18** Linear Dichroism spectra at pH 6.0 (red) and pH 8.0 (blue) for MC/MCH with DNA for **8** (left) and **9** (right).

LD was used to derive information about the binding mode. The reduced LD,  $LD^r$ , was calculated from the absorbance of the bound species for each LD spectrum. The corresponding isotropic absorbance as well as  $LD^r$  can be seen in Figure 5.19.

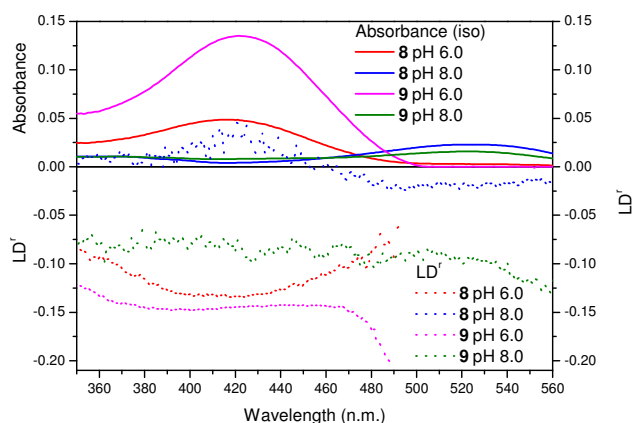


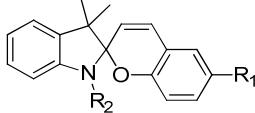
**Figure 5.19** Isotropic absorbance and the corresponding  $LD^r$

With an  $LD^r$  of -0.23 (not seen) of DNA in all samples, the same  $LD^r$  of the **8** or **9** corresponds to an orientation very close to the orientation of the bases. If intercalation is suspected, a negative  $LD^r$  should be seen. In this case, the  $LD^r$  is negative even though not as much as -0.23, but almost all spectra are below -0.10. The only spectrum that is rather unique is the MC at pH 8 for **8**. If all the rest of the species have the same binding mode such as intercalation, this one does not however have that. Instead, it is likely to be close to the magic angle where no LD is seen which may correspond to a groove binding. As the species has only one charge at the phenol ring, it is possible that it is the water soluble tail which makes the intercalation possible. As the absorbance of **8** at high pH is unique such that it has the largest red-shift of all the spiropyrans, this may be the case.

## 5.6 Paper VI – Photoswitched Energy Transfer on DNA

Energy transfer between two fluorophores attached to a DNA strand was photonically switched using the interaction of spiropyrans to DNA.

**Table 5.10** Photochromic compound used in Paper VI.

	$R_1$	$R_2$
		
<b>8</b>	$R_1 = \text{C}(\text{NH}_2)=\text{C}^+(\text{NH}_2)$	$R_2 = -\text{CH}_3$

In Paper II we turned *on* and *off* fluorescence via an energy transfer mechanism based on the photochromic SP, MC and MCH forms. In Paper III and Paper V the spiropyran was characterised by its interaction with DNA. Inspired by the combination of these results, we designed a system where the energy transfer would be turned *on* and *off* by the spiropyran DNA interaction using light on a DNA scaffold with attached fluorophores.

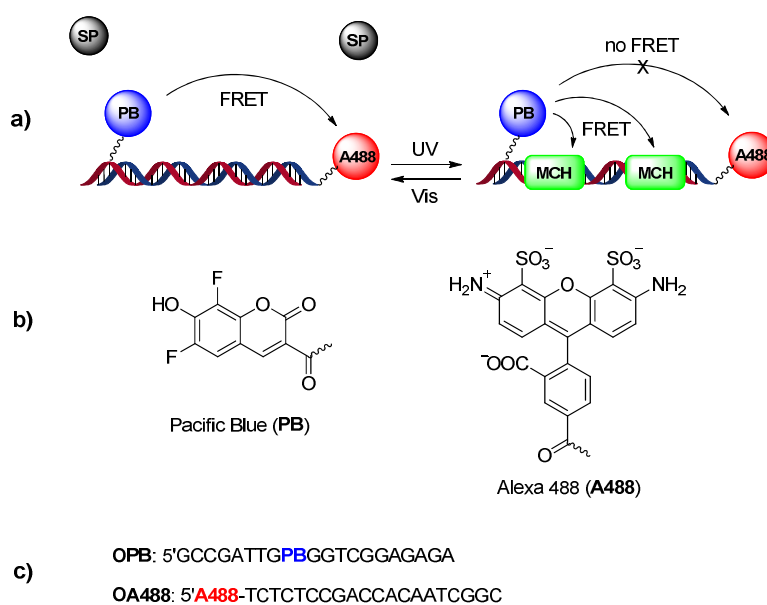


**Figure 5.20** a) Schematic representation of the *on-off* switching of FRET between **BP** and **A488** by reversible isomerisation of spiropyran derivative **8** between the SP and MCH forms. b) Structures of the **PB** and **A488** dyes. c) Sequences of the dye-labeled 20-mer oligonucleotides.

The basic structure is two 20-mer DNA single strands, one with the fluorophore Pacific Blue (**PB**) on a thymine base, one with end-labelled Alexa 488 (**A488**), see Figure 5.20. The fluorophores were chosen based on their well-known fluorescence and absorbance, which make them a great donor-acceptor pair for the Förster mechanism of energy transfer. The strands are complementary and hybridised to form a double strand where **PB** is situated 11 base-pairs away from **A488**, which is well within the calculated Förster distance. Hence, it is very likely that the fluorescence of **PB** will be quenched and **A488** sensitised. However, MCH

which binds to DNA has an absorbance that also overlaps with the emission of **PB** with a very similar calculated Förster distance. Hence, it can also quench the fluorescence of **PB** and if it binds to DNA it is very likely that it will be positioned between **PB** and **A488** on the strand, which will enhance the strongly distance dependent energy transfer. As the binding constant is well-known from Paper V, we pinpointed the concentrations of oligomer as well as **8** to give as large photo-controlled effect as possible.

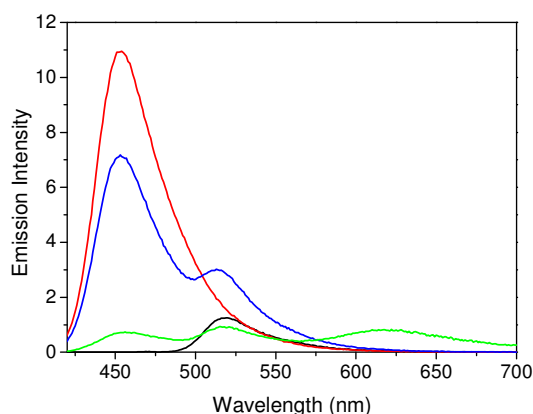


**Figure 5.21** Emission intensities (excitation at 410 nm) for **OPB** (red) and **OA488** (black) hybridised with the respective unlabelled complementary strand. Also shown are the corresponding spectra of the **OPB-OA488** double strand before (blue) and after (green) the addition of 12  $\mu$ M **8** at thermal equilibrium.

In Figure 5.21 fluorescence of the reference oligomers **OA488** and **OPB** are shown. These are the double stranded oligomers of **PB** and **A488**, respectively, alone with an unmodified complementary strand. By excitation at 410 nm, a large emission of **PB** is seen while a much smaller amount of **A488** is excited (due to lower absorbance of **A488** at this wavelength). In the same figure, the fluorescence of the combined strand **OPB-OA488** can be seen where the fluorescence of **PB** is decreased *ca* 37% and with a concomitant sensitisation of the **A488** emission. By addition of **8** at thermal equilibrium where *ca* 80% consists of MC/MCH, it binds to DNA and the resulting fluorescence of **PB** is now quenched down to 3.8%.

The light-controlled switching was investigated by exposure of the sample with 4 min visible light which triggers the switching of MCH and MC to SP. As SP does not bind to DNA and its absorption is well below the emission of **PB**, we expect the fluorescence to increase to its initial state before addition of **8**. Indeed, the fluorescence of **PB**, seen in Figure 5.22, increases and returns almost up to its initial intensity. Hence, we can almost fully turn *off* the energy transfer to **8** with visible light. After this, the sample was irradiated by UV light 3 min to establish a photostationary distribution of MC/MCH of *ca* 20%. As shown in the same figure, this turned on the quenching and the fluorescence from **PB** and **A488** decreased again. Even though the dynamic range is not maximal, we successfully turned *on* and *off* the energy transfer with light.



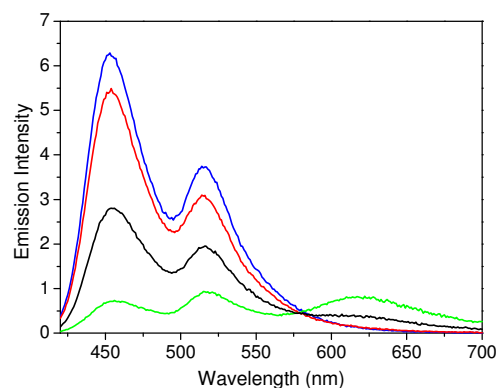


**Figure 5.22** Emission intensities (excitation at 410 nm) for the **OPB-OA488** double strand before (blue) and after (green) the addition of 12  $\mu\text{M}$  **8** at thermal equilibrium. The red line shows the emission intensity after visible light irradiation to isomerise **8** to the non-binding SP form, whereas the black line is the emission after subsequent UV irradiation to isomerise **8** to the DNA-binding MCH form.

After one successful cycle, we repeated the procedure to gain insight into its photostability. As can be seen in Figure 5.23, the operation could be repeated up to 4 times with no significant photo-degradation.

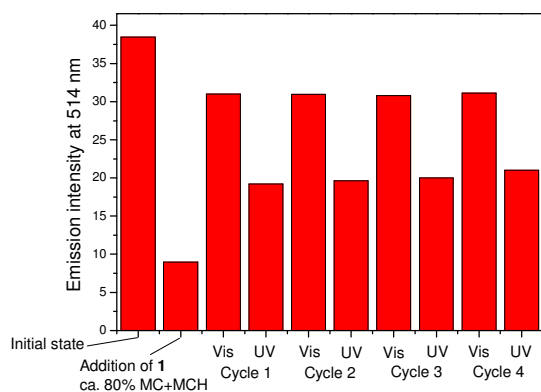


**Figure 5.23** Emission intensity from the **OPB-OA488** double strand at 514 nm after excitation at 410 nm for the relevant situations. Initial state = the **OPB-OA488** double strand before addition of **8**. The exposure times were 3 min. 254 nm UV light and 4 min. visible light ( $\lambda > 450$  nm).

With this, the DNA-binding features of the spiropyran as well as the isomerisation-induced energy transfer quenching was successfully combined to realise photonically controlled energy transfer switching on a DNA scaffold.



---

## 6 Concluding Remarks

---

The aim of this work has been to apply photochromism in molecular logic and biologic contexts, *i.e.* DNA-interaction and aqueous solution behaviour. Paper I and Paper II are examples of applied molecular logic of photochromic compounds where the light input can change properties on the molecular level which affects observable properties applied to conquer the same problems as silicon based devices do today in any electronic equipment. There is obviously space for improvements: The molecular memory could be better if used in the solid state and the sequential AND-gate suffers from poor thermal stability, which implies that the output must be read soon after input application. As stated before, there are many interesting logic gates to design but we are far away from being ready to replace silicon based devices. Instead, the binary schemes of turn *on* and *off* have more use in biological systems where DNA interaction serves as one of these major challenges. The photochromic spiropyrans have been thoroughly characterised in water. We have suggested a mechanism for all thermal processes of spiropyrans, compared it to different modifications of the spiropyran and successfully shown the model to be valid. This gain in knowledge has been applied to DNA binding studies. With a focus on the binding interaction of the open merocyanine form, the results have given a new understanding of how the binding is connected with the protonated form. Still, there are also many more steps to go before it can actually be used as a drug in *e.g.* cancer treatment.

Although photochromism has been shown to be a good tool to be further explored in both logic devices as well as biologic matters, most of the work in this thesis qualifies as so-called proof of principle studies. Many things are possible but in reality there is much left to do before real-world applications can be realised. Still, we must believe that this kind of chemistry will provide more knowledge, in order to give one step in the progress of understanding the world and hopefully make it better. It is in this context that the results of this thesis should be seen.



---

## 7 Acknowledgements

---

I would first of all like to thank my supervisor Joakim Andréasson for your endless support throughout these years together with enjoyable discussions. Thank you for all your help and time!

Thanks to my co-supervisor Per Lincoln for your support and specially the help with the binding studies on DNA.

A special thanks to my co-authors: Joakim – for a memorable moment, Patricia – un momento perfecto en España, Johanna – for all help and discussions, Jesper – always happy and helpful, Magnus – for a fun time in the lab.

Thank you Tamara for nice discussions as well as the proof-reading of this thesis, Patrik for proof-reading this thesis. Bosse – thank you for your support and Shiming thank you for synthesis of the compounds and characterisation in NMR.

Thank you my roommates Maxim, Catherine and David – has been a good time and fun discussions in the room. Thank you all the people on Physical Chemistry – for a genuine and wonderful atmosphere.

Thank you Claes for the long journey in chemistry. Thank you E.T. – I have loved the time together with you. Last but not least, a special thanks for the support from my friends and family. Mamma och Pappa, I finally made it, thank you!



---

## 8 References

---

- [1] A. Einstein, *Phys. Z.* **1909**, *10*, 817.
- [2] Henri Bouas-Laurent, H. Dürr, *Pure Appl. Chem.* **2001**, *73*, 639.
- [3] Y. Hirshberg, E. Fischer, *J. Chem. Soc.* **1953**, 629.
- [4] Y. Hirshberg, E. Fischer, *J. Chem. Soc.* **1954**, 297.
- [5] Y. Hirshberg, E. Fischer, *J. Chem. Soc.* **1954**, 3129.
- [6] M. Irie, *Chem. Rev.* **2000**, *100*, 1683.
- [7] R. C. Bertelson, *Organic Photochromic and Thermochromic Compounds, Vol. 1*, Plenum Press, New York, **1999**.
- [8] J. Chelikowski, *Silicon: evolution and future of a technology*, Springer, **2004**.
- [9] G. E. Moore, *Electronics* **1965**, *38*, 114.
- [10] CORDIS, **2005**.
- [11] A. C. V. Balzani, M. Venturi, *Molecular Devices and Machines. Concepts and Perspectives for the Nanoworld*, 2nd ed. ed., Wiley-VCH, Weinheim, **2008**.
- [12] A. P. de Silva, Gunaratne, H. Q. N., McCoy, C.P., *Nature* **1993**, *364*, 42.
- [13] V. Balzani, A. Credi, M. Venturi, *ChemPhysChem* **2003**, *4*, 49.
- [14] A. P. de Silva, S. Uchiyama, *Nat. Nanotechnol.* **2007**, *2*, 399.
- [15] K. Szacilowski, *Chem. Rev.* **2008**, *108*, 3481.
- [16] J. Andréasson, U. Pischel, *Chem. Soc. Rev.* **2010**, *39*, 174.
- [17] F. M. Raymo, *Adv. Mater.* **2002**, *14*, 401.
- [18] J. Andréasson, S. D. Straight, G. Kodis, C. D. Park, M. Hambourger, M. Gervaldo, B. Albinsson, T. A. Moore, A. L. Moore, D. Gust, *JACS* **2006**, *128*, 16259.
- [19] M. N. Stojanovic, D. Stefanovic, *JACS* **2003**, *125*, 6673.
- [20] D. H. Qu, Q. C. Wang, H. Tian, *Angew. Chem. Int. Ed.* **2005**, *44*, 5296.
- [21] J. Andréasson, S. D. Straight, T. A. Moore, A. L. Moore, D. Gust, *JACS* **2008**, *130*, 11122.
- [22] P. Ceroni, G. Bergamini, V. Balzani, *Angew. Chem. Int. Ed.* **2009**, *48*, 8516.
- [23] F. M. Raymo, M. Tomasulo, *J. Phys. Chem. A* **2005**, *109*, 7343.
- [24] F. M. Raymo, M. Tomasulo, *Chem. Soc. Rev.* **2005**, *34*, 327.
- [25] J. Cusido, E. Deniz, F. M. Raymo, *Eur. J. Org. Chem.* **2009**, 2031.
- [26] R. J. Amir, M. Popkov, R. A. Lerner, C. F. Barbas III, D. Shabat, *Angew. Chem. Int. Ed.* **2005**, *44*, 4378.
- [27] S. Angelos, Y.-W. Yang, N. M. Khashab, J. F. Stoddart, J. I. Zink, *JACS* **2009**, *131*, 11344.
- [28] T. Konry, D. R. Walt, *JACS* **2009**, *131*, 13232.
- [29] S. Muramatsu, K. Kinbara, H. Taguchi, N. Ishii, T. Aida, *JACS* **2006**, *128*, 3764.
- [30] S. Ozlem, E. U. Akkaya, *JACS* **2009**, *131*, 48.
- [31] O. Warburg, *Science* **1956**, *123*, 309.
- [32] P. Montcourrier, P. H. Mangeat, C. Valembois, G. Salazar, A. Sahuquet, C. Duperray, H. Rochefort, *J. Cell Sci.* **1994**, *107*, 2381.
- [33] I. L. Cameron, N. K. R. Smith, T. B. Pool, R. L. Sparks, *Cancer Res.* **1980**, *40*, 1493.
- [34] F. Crick, *Nature* **1970**, *227*, 561.
- [35] J. D. Watson, F. H. C. Crick, *Nature* **1953**, *171*, 737.
- [36] R. Wing, H. Drew, T. Takano, C. Broka, S. Tanaka, K. Itakura, R. E. Dickerson, *Nature* **1980**, *287*, 755.
- [37] W. H. Braunlin, T. J. Strick, M. T. Record, *Biopolymers* **1982**, *21*, 1301.

- [38] A. J. Bruce Alberts, Julian Lewis, Martin Raff, Keith Roberts, Peter Walter, *Molecular Biology of the Cell*, Fourth Edition ed., Garland Science, New York, **2002**.
- [39] H. Asanuma, T. Ito, T. Yoshida, X. G. Liang, M. Komiyama, *Angew. Chem. Int. Ed.* **1999**, *38*, 2393.
- [40] H. Nishioka, X. G. Liang, H. Kashida, H. Asanuma, *Chem. Commun.* **2007**, 4354.
- [41] H. Asanuma, T. Takarada, T. Yoshida, D. Tamaru, X. G. Liang, M. Komiyama, *Angew. Chem. Int. Ed.* **2001**, *40*, 2671.
- [42] A. Yamazawa, X. G. Liang, H. Asanuma, M. Komiyama, *Angew. Chem. Int. Ed.* **2000**, *39*, 2356.
- [43] M. Z. Liu, H. Asanuma, M. Komiyama, *JACS* **2006**, *128*, 1009.
- [44] H. Cahova, A. Jaeschke, *Angew. Chem. Int. Ed.* **2013**, *52*, 3186.
- [45] G. W. T. M. J. Frisch, H. B. Schlegel, G. E. Scuseria, M. A. Robb, J. R. Cheeseman, J. A. Montgomery, Jr., T. Vreven, K. N. Kudin, J. C. Burant, J. M. Millam, S. S. Iyengar, J. Tomasi, V. Barone, B. Mennucci, M. Cossi, G. Scalmani, N. Rega, G. A. Petersson, H. Nakatsuji, M. Hada, M. Ehara, K. Toyota, R. Fukuda, J. Hasegawa, M. Ishida, T. Nakajima, Y. Honda, O. Kitao, H. Nakai, M. Klene, X. Li, J. E. Knox, H. P. Hratchian, J. B. Cross, V. Bakken, C. Adamo, J. Jaramillo, R. Gomperts, R. E. Stratmann, O. Yazyev, A. J. Austin, R. Cammi, C. Pomelli, J. W. Ochterski, P. Y. Ayala, K. Morokuma, G. A. Voth, P. Salvador, J. J. Dannenberg, V. G. Zakrzewski, S. Dapprich, A. D. Daniels, M. C. Strain, O. Farkas, D. K. Malick, A. D. Rabuck, K. Raghavachari, J. B. Foresman, J. V. Ortiz, Q. Cui, A. G. Baboul, S. Clifford, J. Cioslowski, B. B. Stefanov, G. Liu, A. Liashenko, P. Piskorz, I. Komaromi, R. L. Martin, D. J. Fox, T. Keith, M. A. Al-Laham, C. Y. Peng, A. Nanayakkara, M. Challacombe, P. M. W. Gill, B. Johnson, W. Chen, M. W. Wong, C. Gonzalez, J. A. Pople, *Gaussian 03, Revision B.05*, Gaussian, Inc., Pittsburgh PA, **2003**.
- [46] D. D. Young, A. Deiters, *ChemBioChem* **2008**, *9*, 1225.
- [47] D. Berdnikova, O. Fedorova, E. Gulakova, H. Ihmels, *Chem. Commun.* **2012**, *48*, 4603.
- [48] C. Dohno, S. N. Uno, K. Nakatani, *JACS* **2007**, *129*, 11898.
- [49] C. Dohno, S. N. Uno, S. Sakai, M. Oku, K. Nakatani, *Biorg. Med. Chem.* **2009**, *17*, 2536.
- [50] C. Dohno, T. Yamamoto, K. Nakatani, *Eur. J. Org. Chem.* **2009**, 4051.
- [51] J. Andersson, S. M. Li, P. Lincoln, J. Andréasson, *JACS* **2008**, *130*, 11836.
- [52] F. Jonsson, T. Beke-Somfai, J. Andreasson, B. Norden, *Langmuir* **2013**, *29*, 2099.
- [53] J. R. Nilsson, S. M. Li, B. Onfelt, J. Andreasson, *Chem. Commun.* **2011**, *47*, 11020.
- [54] C. Brieke, F. Rohrbach, A. Gottschalk, G. Mayer, A. Heckel, *Angew. Chem. Int. Ed.* **2012**, *51*, 8446.
- [55] G. Mayer, A. Heckel, *Angew. Chem. Int. Ed.* **2006**, *45*, 4900.
- [56] I. Willner, S. Rubin, *Angew. Chem. Int. Ed. Engl.* **1996**, *35*, 367.
- [57] A. Rodger, B. Nordén, *Circular Dichroism and Linear Dichroism*, Oxford University Press, Oxford, **1997**.
- [58] B. Nordén, *Applied Spectroscopy Reviews* **1978**, *14*, 157.
- [59] D. L. Dexter, *J. Chem. Phys.* **1953**, *21*, 836.
- [60] N. J. Turro, *Pure Appl. Chem.* **1977**, *49*, 405.
- [61] T. Förster, *Naturwissenschaften* **1946**, *33*, 166.
- [62] T. Förster, *Annalen Der Physik* **1948**, *2*, 55.
- [63] M. Kubista, R. Sjoback, B. Albinsson, *Anal. Chem.* **1993**, *65*, 994.
- [64] J. D. McGhee, P. H. V. Hippel, *J. Mol. Biol.* **1974**, *86*, 469.
- [65] G. H. Brown, *Photochromism*, Wiley, New York, **1971**.



- [66] S. V. Paramonov, V. Lokshin, O. A. Fedorova, *J. Photochem. Photobiol., C* **2011**, *12*, 209.
- [67] J. W. Zhou, Y. T. Li, Y. W. Tang, F. Q. Zhao, X. Q. Song, E. C. Li, *J. Photochem. Photobiol., A* **1995**, *90*, 117.
- [68] K. Namba, S. Suzuki, *Bull. Chem. Soc. Jpn.* **1975**, *48*, 1323.
- [69] T. Stafforst, D. Hilvert, *Chem. Commun.* **2009**, 287.
- [70] Y. Shiraishi, M. Itoh, T. Hirai, *Phys. Chem. Chem. Phys.* **2010**, *12*, 13737.
- [71] R. Li, C. S. Santos, T. B. Norsten, K. Morimitsu, C. Bohne, *Chem. Commun.* **2010**, 46, 1941.
- [72] Y. Shiraishi, M. Itoh, T. Hirai, *Tetrahedron Lett.* **2011**, *52*, 1515.
- [73] J. Kohl-Landgraf, M. Braun, C. Ozcoban, D. P. N. Goncalves, A. Heckel, J. Wachtveietl, *JACS* **2012**, *134*, 14070.
- [74] Y. Shiraishi, K. Tanaka, T. Hirai, *ACS Appl. Mater. Interfaces* **2013**, *5*, 3456.
- [75] M. Irie, *Chem. Rev.* **2000**, *100*, 1685.
- [76] M. Irie, M. Mohri, *J. Org. Chem.* **1988**, *53*, 803.
- [77] M. Hanazawa, R. Sumiya, Y. Horikawa, M. Irie, *J. Chem. Soc., Chem. Commun* **1992**, 206.
- [78] T. C. S. Pace, V. Muller, S. Li, P. Lincoln, J. Andréasson, *Angew. Chem. Int. Ed.* **2013**, *52*, 4393.
- [79] M. U. Winters, J. Karnbratt, M. Eng, C. J. Wilson, H. L. Anderson, B. Albinsson, *J. Phys. Chem. C* **2007**, *111*, 7192.
- [80] M. U. Winters, J. Karnbratt, H. E. Blades, C. J. Wilson, M. J. Frampton, H. L. Anderson, B. Albinsson, *Chem.--Eur. J.* **2007**, *13*, 7385.
- [81] J. T. C. Wojtyk, A. Wasey, N.-N. Xiao, P. M. Kazmaier, S. Hoz, C. Yu, R. P. Lemieux, E. Buncel, *J. Phys. Chem. A* **2007**, *111*, 2511.
- [82] Z. Miskolczy, L. Biczok, *J. Phys. Chem. B* **2011**, *115*, 12577.
- [83] Z. Miskolczy, L. Biczok, *J. Phys. Chem. B* **2013**, *117*, 648.
- [84] J. Kohl-Landgraf, M. Braun, C. Ozcoban, D. P. N. Goncalves, A. Heckel, J. Wachtveietl, *JACS* **2012**, *134*, 14070.
- [85] J. Andraos, *J. Chem. Educ.* **1999**, *76*, 1578.
- [86] K. C. Gross, P. G. Seybold, *Int. J. Quant. Chem.* **2001**, *85*, 569.
- [87] W. D. Wilson, F. A. Tanious, D. Y. Ding, A. Kumar, D. W. Boykin, P. Colson, C. Houssier, C. Bailly, *JACS* **1998**, *120*, 10310.
- [88] S. Ozden, D. Atabey, S. Yildiz, H. Goker, *Biorg. Med. Chem.* **2005**, *13*, 1587.
- [89] V. Brabec, E. Palecek, *Biophysik* **1970**, *6*, 290.
- [90] Costanti.L, Vitaglia.V, *Biopolymers* **1966**, *4*, 521.
- [91] E. L. Duggan, V. L. Stevens, B. W. Grunbaum, *JACS* **1957**, *79*, 4859.
- [92] R. M. Kothari, *J. Chromatogr.* **1971**, *59*, 194.
- [93] J. Sturm, J. Lang, R. Zana, *Biopolymers* **1971**, *10*, 2639.